

How Old Is It?

Part 2 – Magnetostratigraphy

Introduction

In addition to biostratigraphy, the stratigraphic record of the episodic reversals of Earth's magnetic field is another tool to establish a stratigraphy and provide age information for cored crustal rocks, intrusions, and sedimentary sequences. This is just one attribute of the magnetic signature preserved in sediments or oceanic crust (basalt) that can tell us about the changing nature of Earth's magnetic field through time.

The magnetic signal that geoscientists are interested in measuring is called natural remanent magnetization (NRM). This signal is carried by magnetic minerals such as magnetite. The NRM is preserved in basalt as it cools and crystallizes past the Curie temperature ($\sim 580^{\circ}\text{C}$ for the mineral magnetite), or in sediments as detrital magnetic mineral grains accumulate on the seafloor. In both situations, the magnetic minerals become aligned with the Earth's magnetic field at the time of crystallization and deposition, respectively.

Not all rocks are good carriers of a magnetic signal. The basalt that makes up oceanic crust is a magnetite-bearing rock, while granite, a typical igneous rock of continental crust, is generally poor in magnetic minerals. Likewise, marine sediments composed of terrigenous silt and clay derived from the erosion of continental rocks have a much higher concentration of detrital magnetic mineral grains than does a pure biogenic sediment, such as calcareous or siliceous ooze.

Describe the Earth's magnetic field. What are the key features or characteristics of our magnetic field? A sketch may help.

Earth's Magnetic Field

Earth's magnetic field is somewhat analogous to a bar magnet, in that the field is a dipole with a north pole and a south pole. The magnetic field is induced by an electromagnetic current created by fluid motion in the liquid outer core due to Earth's rotation. The north and south magnetic poles are close to Earth's rotational axis, the latter represented by the geographic North Pole and South Pole, but Magnetic North and Magnetic South are offset from true North and true South.

Earth's magnetic field is dynamic and complex. The magnetic poles are not stationary. In 2005, the north magnetic pole was at 82.7°N , 114.4°W , moving northwest at approximately 40 km/yr, while the south magnetic pole (2001) was at 64.7°S , 138.0°E (www.ngdc.noaa.gov/seg/geomag/faggeom.shtml).

In addition, Earth's magnetic field episodically reverses polarity. Prior to a reversal of the magnetic field, the field randomizes and becomes weaker, and there may be multiple poles for a short time. The pro-

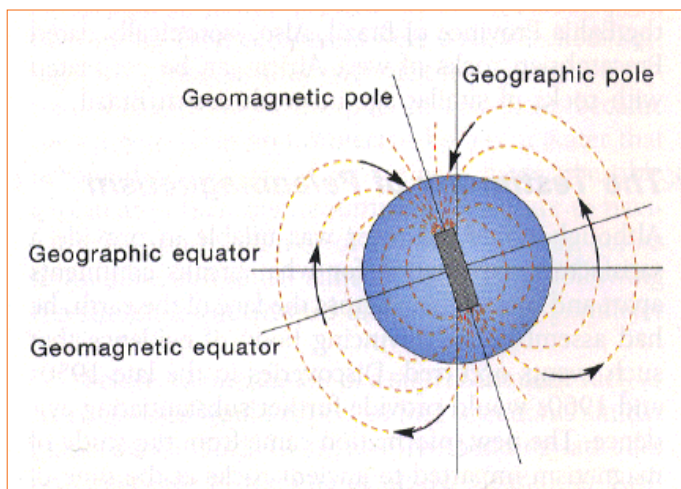


Figure 1. Earth's magnetic field under "normal polarity". The arrows depicting magnetic lines of force would be oriented in the opposite direction with a reversed field (reversed polarity). Figure from <http://www.geocities.com/CapeCanaveral/Lab/6488/magfield.html>.

cess is geologically rapid, taking several thousand years for the field to completely reverse polarity and stabilize again. Today's field is referred to as "normal polarity" (Figure 1). The last reversal of the magnetic field occurred approximately 780,000 years ago. Refer to <http://www.ngdc.noaa.gov/seg/geomag/faqqgeom.shtml#q1> for additional information about Earth's magnetic field.

The ancient magnetic field (paleomagnetism) is measured in rocks and sediments using a magnetometer. See <http://www-odp.tamu.edu/sciops/labs/pmag/> for a detailed discussion of how shipboard paleomagnetic data are collected.

Activity

The figures below depict the magnetic character

of two deep-sea sediment cores. Site 1149 (Figure 2a) is located in the northwest Pacific (~31°N latitude) near the Marianas Trench. Site 1172 (Figure 2b) is located in the southwest Pacific (~44°S latitude) near Tasmania. Both records have been interpreted by correlating to the late Cenozoic Geomagnetic Polarity Time Scale (Berggren et al., 1995; Cande and Kent, 1995).

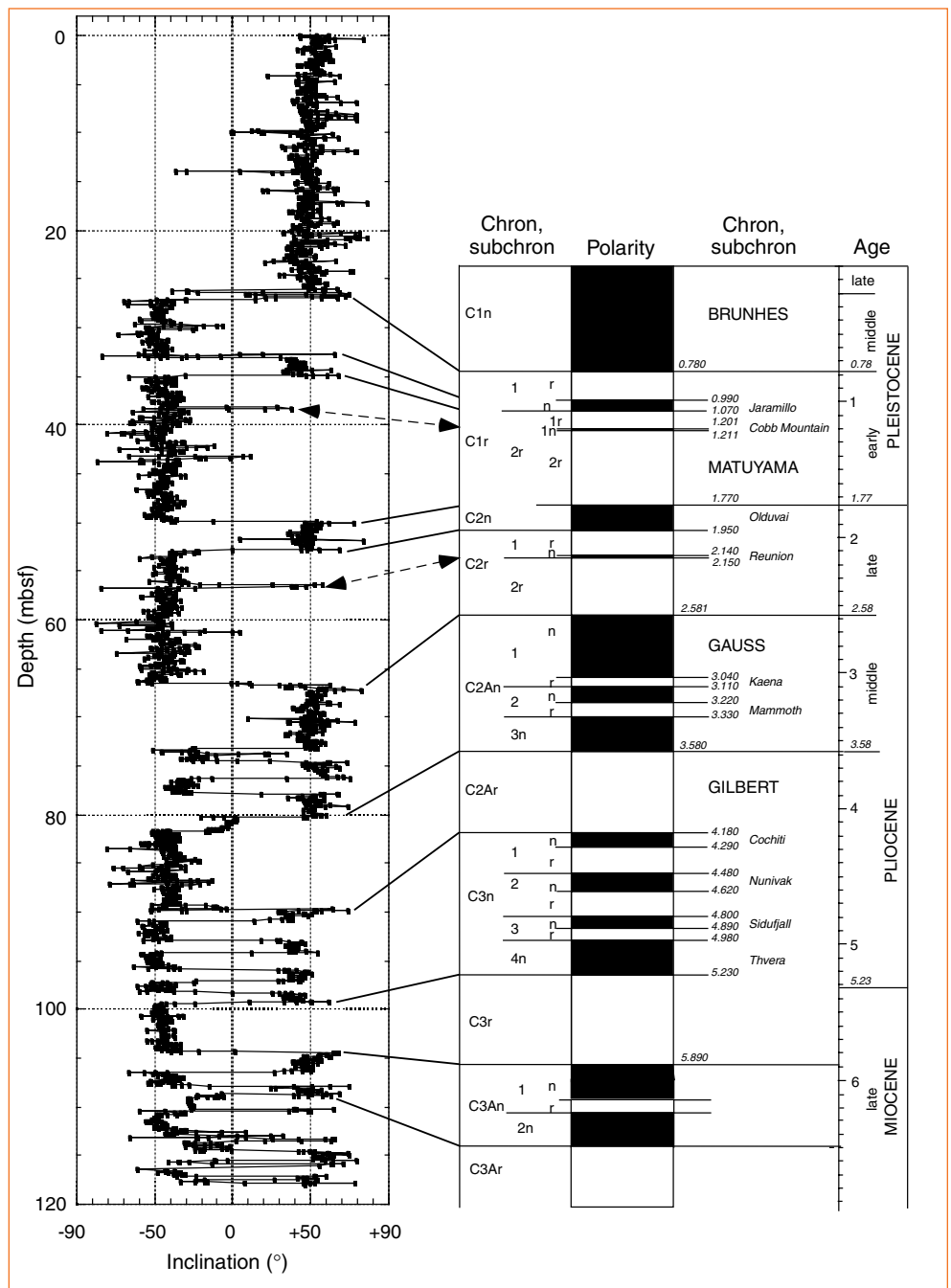
Make a list of observations about the paleomagnetic record in these two deep-sea sediment sequences. How are they similar, and how are they different?

Figure 2a. Interpreted paleomagnetic stratigraphy from Site 185-1149 in the northwest Pacific (31°20.095'N, 143°21.805'E; 5817 m water depth). http://www-odp.tamu.edu/publications/185_IR/chap_04/c4_f66.htm#573212.

The Nature of the Earth's Magnetic Field as Recorded in Sediments and Rocks

There are two ancient field directions typically preserved in sedimentary or igneous rocks containing magnetic minerals. A reversal of the magnetic field is seen as an abrupt change in these directions. Plate motion over time also affects the field directions preserved in rocks. Inclination, or magnetic dip, represents the angle of magnetization into or out of the Earth's surface (Figures 1 and 3).

The magnetic lines of force are directed into the Earth in the Northern Hemisphere (positive down), and directed out of the Earth in the Southern Hemisphere (positive up; magnetic field is oriented upwards). In other words, today's magnetic field (=



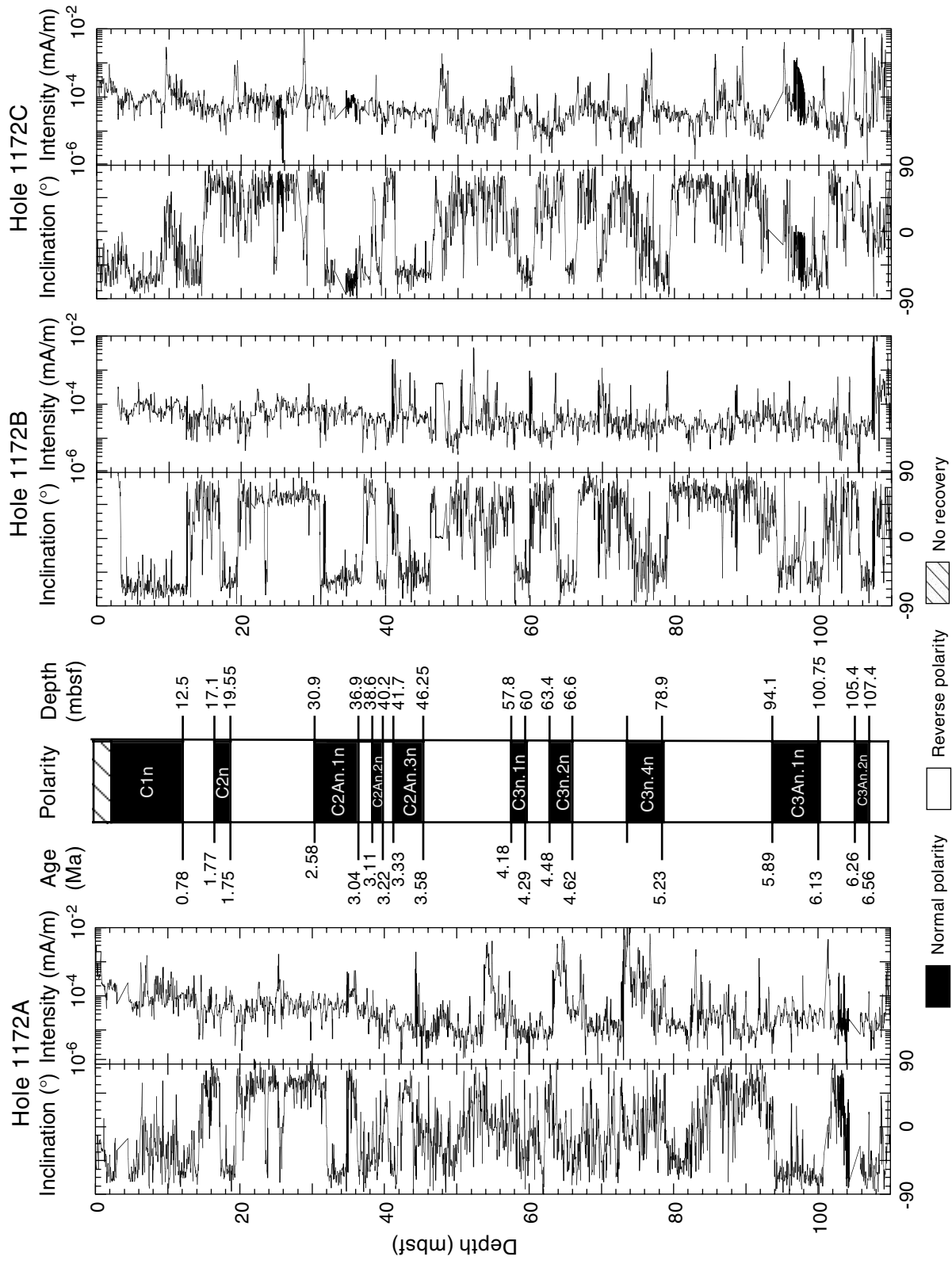


Figure 2b. Interpreted paleomagnetic stratigraphy from Site 189-1172 in the southwest Pacific (43°57.575'S, 149°55.701'E; 2622 m water depth). From http://www-odp.tamu.edu/publications/189_IR/chap_07/c7_f16.htm#382526.

“normal polarity”) is represented by positive inclination in the Northern Hemisphere, and by negative inclination in the Southern Hemisphere.

Near the equator, the magnetic lines of force are parallel to the Earth’s surface. In this way, magnetic inclination is a function of latitude; $\sim 90^\circ$ inclination at the north and south magnetic pole, $\sim 0^\circ$ at the equator, and intermediate values in between. Inclination is used to determine the paleolatitude of igneous or sedimentary rocks and sediments at the time of crystallization or deposition.

Declination, or azimuth, is the angle between true north and the horizontal trace of the magnetic field for your location (Figure 4). It represents the direction of magnetization (today’s field is in a northerly direction (+/- 0°), whereas during a reversed field, the declination would be in a southerly direction (+/- 180°). Declination can only be determined on sediment cores that have been oriented during coring with respect to the present day magnetic field using the Tensor tool.

The inclination and declination data collected on rock or sediment cores can be used to determine the ancient polarity of the earth, or paleomagnetism. Inclination data are widely used for paleomagnetic studies. However, near the equator, paleomagnetists rely heavily on declination data because inclination is so low. See the Integrated Ocean Drilling Program (IODP) document describing the Paleomagnetism Laboratory aboard the *JOIDES Resolution* for a discussion of magnetic overprinting and what demagnetization techniques are used to remove this overprint from deep-sea cores (http://www.oceanleadership.org/learning/classroom/lab_briefs.html).

Development of the Geomagnetic Polarity Time Scale (GPTS)

Sequences of magnetic reversals measured in deep-sea cores can be correlated with the Geomagnetic Polarity Time Scale (GPTS) in order to determine the age and sedimentation history of a drill site (Figure 5). The Geomagnetic Polarity Time Scale is based on the marine magnetic anomaly sequence recorded in the South Atlantic Ocean, which has then been compared with other ocean basin sequences (Cande and Kent, 1992, 1995). This is the currently accepted GPTS for the later part of the Cretaceous Period and Cenozoic Era (0-84 Ma; Ma = mega-annums). Nine radiometric age tie points, plus the zero-age ridge axis, are used to calibrate this part of the timescale (ages for the marine magnetic anomalies between the calibration points are interpolated by a cubic spline function; Berggren et al., 1995).

Ships towing magnetometers across the ocean basins during the post-WWII era recorded patterns of greater and lesser magnetic intensity relative to the present field. These positive and negative magnetic anomalies represent linear bands of alternating polarity that trend parallel to the spreading axis with a mirror image pattern on the opposite side of the ridge. The positive anomalies correspond with a magnetic polarity as today which amplifies the magnetic intensity, while the negative anomalies correspond with a reversed polarity, which partially dampens out the influence of the present-day field. These observations led to a test of the seafloor spreading hypothesis (Vine and Matthews, 1963; Morley, 1963) advanced by Dietz (1961) and Hess (1962). Heirtzler et al. (1968) created the first GPTS by correlating a single marine magnetic anomaly profile from the South Atlantic to radiometrically dated terrestrial reversal sequences.

For the Late Cretaceous to present, the prominent positive anomalies (i.e., those corresponding to time intervals, or chrons, of normal geomagnetic polarity) have been numbered from Chron 1n in the central axis of the spreading centers to Chron 34n at the younger end of the Cretaceous Long Normal (also called the Cretaceous Quiet Zone; 83.5 Ma). The suffix “n” after the anomaly number refers to normal polarity, and the “r” refers to reversed polarity. Many of the younger chrons are divided into shorter polarity intervals, or subchrons.

The GPTS based on marine magnetic anomalies extends back through the late Middle Jurassic (Callovian stage, ~ 162 Ma; e.g., Kent and Gradstein, 1986), while land-based polarity records go back through the Triassic (e.g., Gradstein et al., 1995). A nomenclature called the “M-sequence” is used for marine magnetic polarity chrons of the Early Cretaceous to late Middle Jurassic extending from Chron M0r at the base the Cretaceous Long Normal (Chron 34n; base of the Aptian stage in the Early Cretaceous, ~ 121 Ma) to Chron M39 in the Jurassic (Callovian stage).

Berggren et al. (1995) correlated Cenozoic calcareous microfossil datum events (calcareous nanofossil and planktic foraminifera) and zonations to the GPTS, which serves as the modern standard for biochronology of the past 65 million years (Figure 6). Astrochronologic calibration (“orbital tuning”) of the GPTS polarity boundaries based on Milankovitch cyclicity in continuous marine sections with excellent magneto- and biostratigraphy has been applied to the Pliocene and Pleistocene (Berggren et al., 1995, and references therein) and older Neogene sequences (e.g., Gradstein, Ogg,

Smith et al., 2004, and references therein). More recently, the International Commission on Stratigraphic has published the latest time scale for the Phanerozoic Eon, which succeeds the 1989 Harland et al. timescale (Gradstein, Ogg, Smith et al., 2004; <http://www.stratigraphy.org>).

Examples of paleomagnetic data collected from two Ocean Drilling Program sites and their interpretations (correlation to the Geomagnetic Polarity Timescale) are shown in Figures 7 and 9. These data provide excellent age control for the two sites. Age-depth plots based on the paleomagnetic reversal ages are shown in Figures 8 and 10. Age-depth plots are used to quantify and graphically depict the sedimentation rate history of the sites.

References

- Berggren, W.A., Kent, D.V., Swisher, C.C., III, and Aubry, M.-P., 1995. A revised Cenozoic geochronology and chronostratigraphy. In, *Geochronology, Time Scales, and Global Stratigraphic Correlation*, SEPM (Society for Sedimentary Geology) Special Publication 54, p. 129-212.
- Cande, S.C., and Kent, D.V., 1992. A new geomagnetic polarity time scale for the Late Cretaceous and Cenozoic. *Journal of Geophysical Research*, 97:13,917-13,951.
- Cande, S.C., and Kent, D.V., 1995. Revised calibration of the geomagnetic polarity timescale for the late Cretaceous and Cenozoic. *Journal of Geophysical Research*, 100:6093-6095.
- Dietz, R.S., 1961. Continent and ocean basin evolution by spreading of the sea floor. *Nature*, 190:854-857.
- Gradstein, F.M., Agterberg, F.P., Ogg, J.G., Hardenbol, J., Van Veen, P., Thierry, J., and Huang, Z., 1995. A Triassic, Jurassic, and Cretaceous time scale. In, *Geochronology, Time Scales, and Global Stratigraphic Correlation*, SEPM (Society for Sedimentary Geology) Special Publication 54, p. 95-126.
- Gradstein, F.M., Ogg, J.G., Smith, A.G., et al., 2004. *Geologic Time Scale 2004*. International Commission on Stratigraphy, Cambridge University Press, 500 p.
- Harland, W.B., Armstrong, R.L., Cox, A.V., Craig, L.E., Smith, A.G., and Smith, D.G., 1990. *A Geologic Time Scale 1989*. Cambridge University Press, 263 p.
- Heirtzler, J.R., Dickson, G.O., Herron, E.M., Pittman, W.C., III, and LePichon, X., 1968. Marine magnetic anomalies, geomagnetic field reversals, and motions of the ocean floor and continents. *Journal of Geophysical Research*, 73:2119-2136.
- Hess, H.H., 1962. *History of the ocean basins*. In, *Petrologic Studies, A Volume in Honor of A.F. Buddington*, Geological Society of America, p. 599-620
- Kent, D.V., and Gradstein, F.M., 1986. A Jurassic to recent chronology. In, *The Geology of North America, Western North Atlantic Region, Volume M*, Geological Society of America, p. 45-50.
- Vine, F.J., and Matthews, D.H., 1963. Magnetic anomalies over oceanic ridges. *Nature*, 199:947-949.

Activity by

Kristen St. John, James Madison University (stjohnke@jmu.edu), and

R. Mark Leckie, University of Massachusetts-Amherst (mleckie@geo.umass.edu).

Adapted from School of Rock materials by Leckie and St. John, 2005.

US/UK World Magnetic Chart -- Epoch 2000 Inclination - Main Field (I)

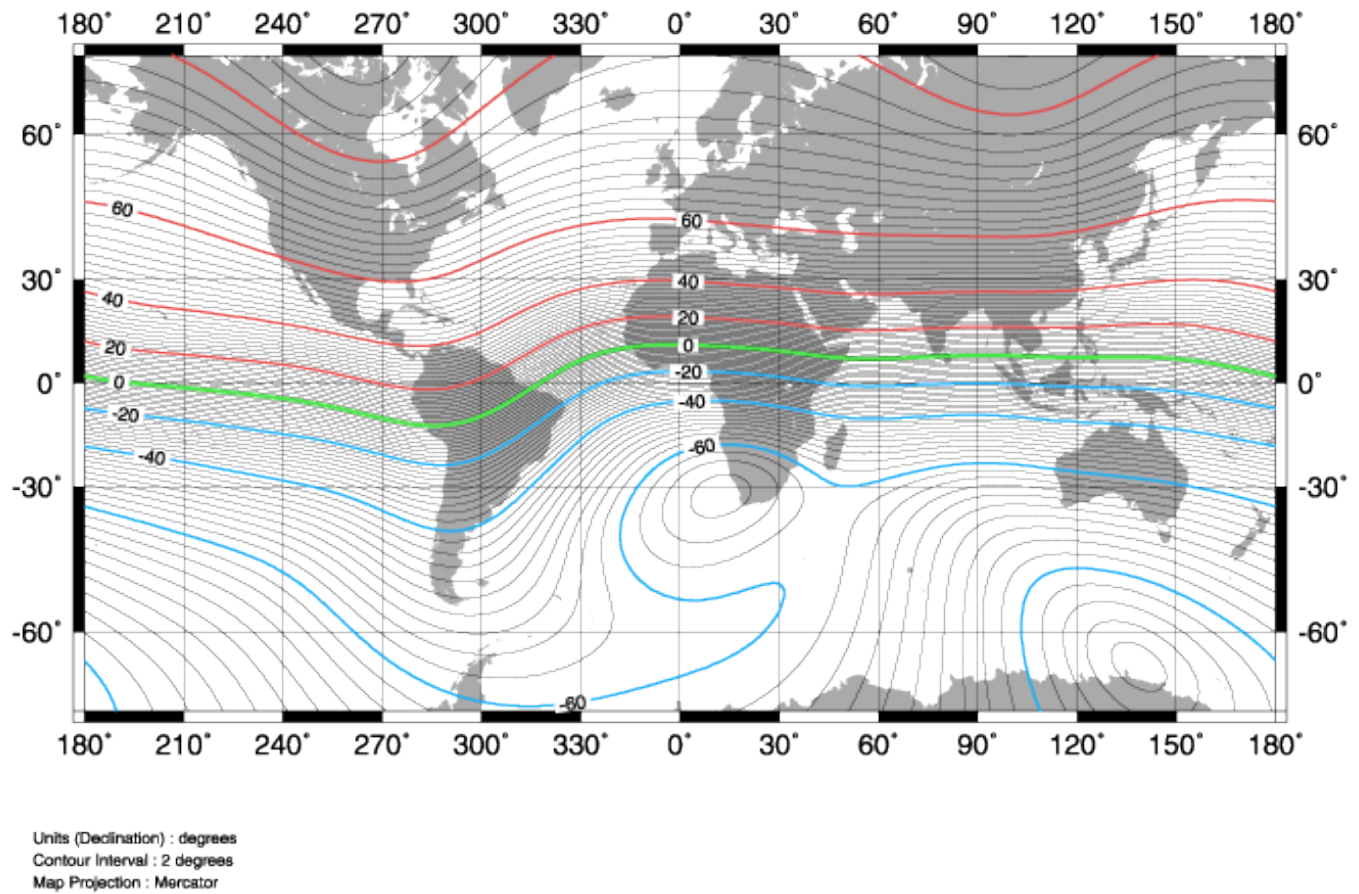


Figure 3. Inclination in the Earth's magnetic field. (<http://www.ngdc.noaa.gov/seg/geomag/icons/wmm2000i.gif>)

US/UK World Magnetic Chart -- Epoch 2000 Declination - Main Field (D)

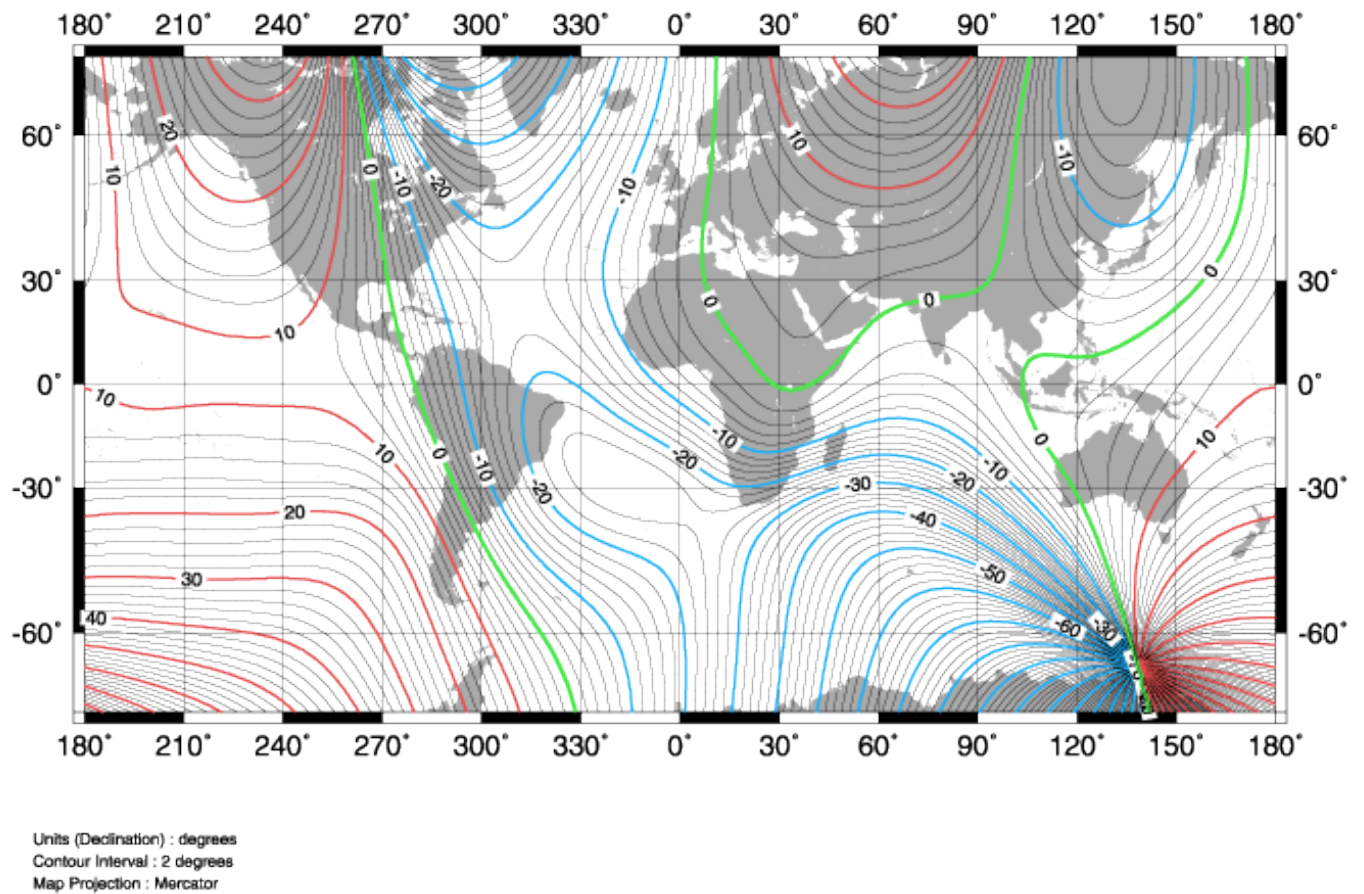


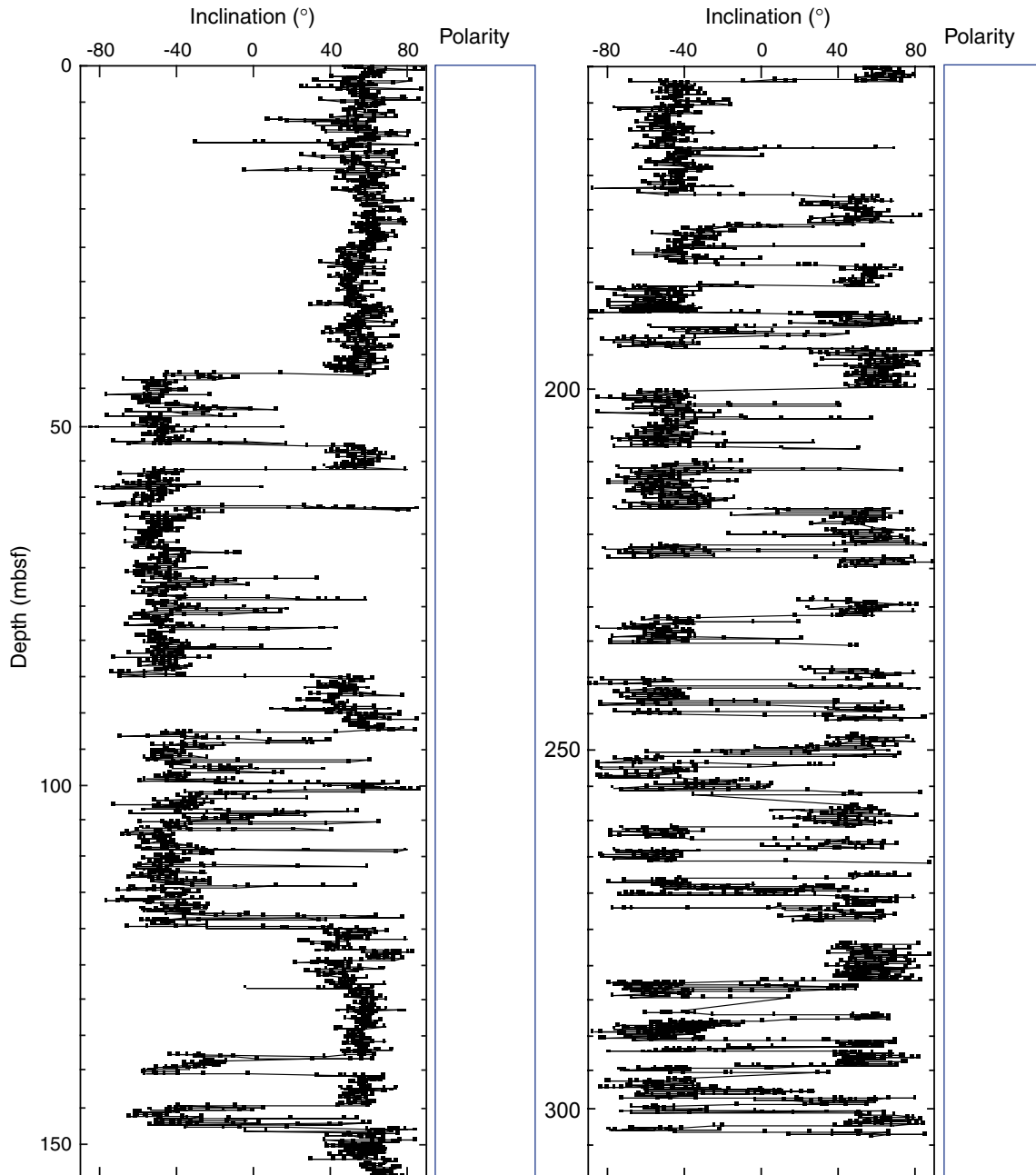
Figure 4. Declination in Earth's magnetic field. (<http://www.ngdc.noaa.gov/seg/geomag/icons/WMM-00D.gif>)

Interpreting the Paleomagnetic Record Preserved in Deep-Sea Sediments

Use Figure 4 to interpret the paleomagnetic stratigraphy (chrons and subchrons) recorded at Site 1208 (below) in the northwest Pacific (Shatsky Rise). What assumptions must you make if you simply correlate the magnetic reversal pattern preserved in Site 1208 with the Geomagnetic Polarity Time Scale shown in Figure 4?

Activity

Examine Figure 4. Make a list of observations about the character of the Earth’s magnetic field over the last 17 million years.



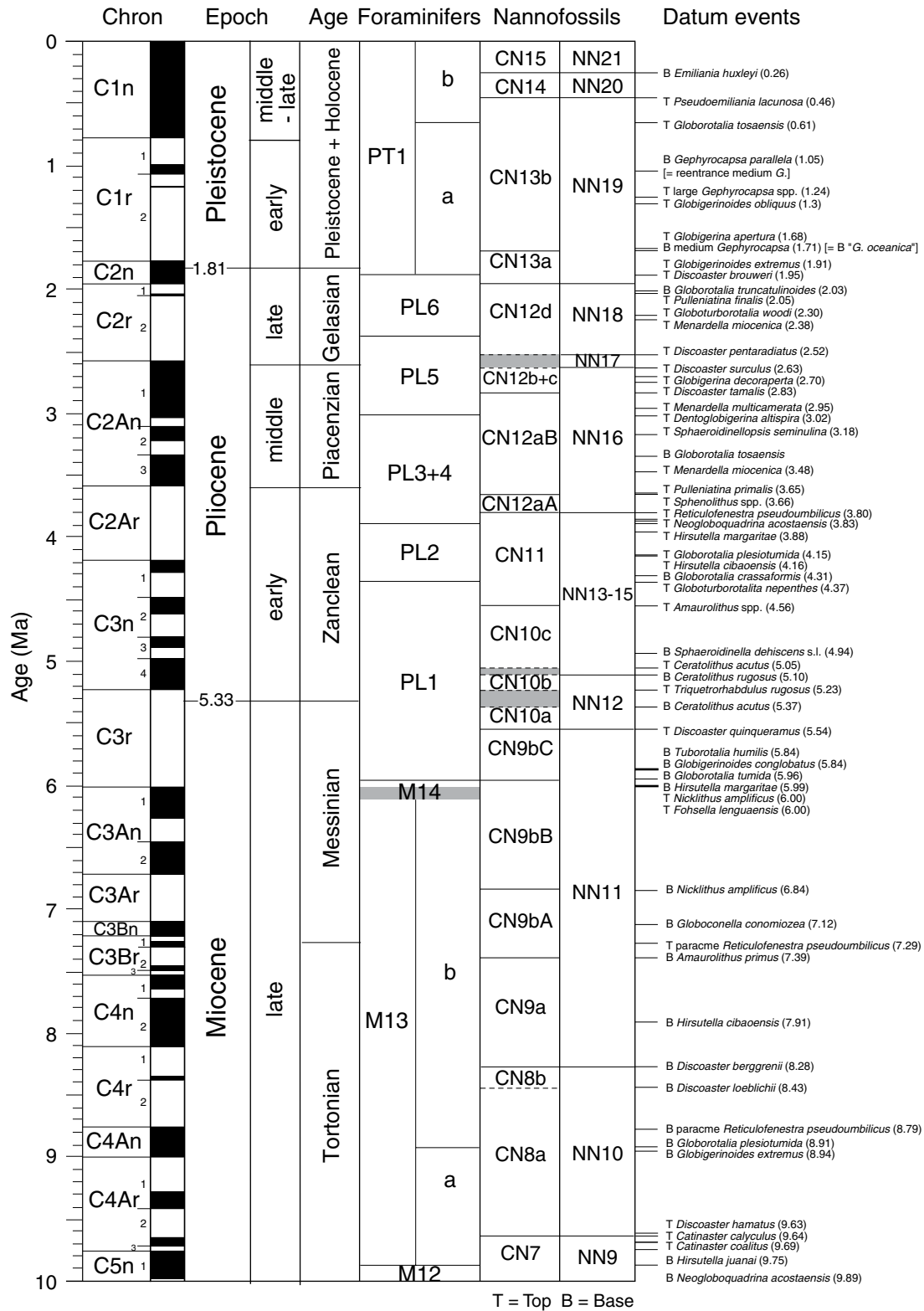


Figure 6.(page 1 of three pages) Integration of biostratigraphy and magnetostratigraphy. Calcareous nannofossil and planktonic foraminiferal zonation used during ODP Leg 208. Use this as a reference for the exercise that follows. References are cited in the text for each microfossil group. Shaded bands with dashed lines indicate that the zonal boundaries are not clearly delimited. T = top, or last occurrence (LO) datum; B = base, or first occurrence (FO) datum; TC = top of common occurrence, BC = bottom of common occurrence. CK95 = Cande and Kent, 1995. From ODP Leg 208 Initial Reports volume, Explanatory Notes chapter, (http://www-odp.tamu.edu/publications/208_IR/chap_02/chap_02.htm)

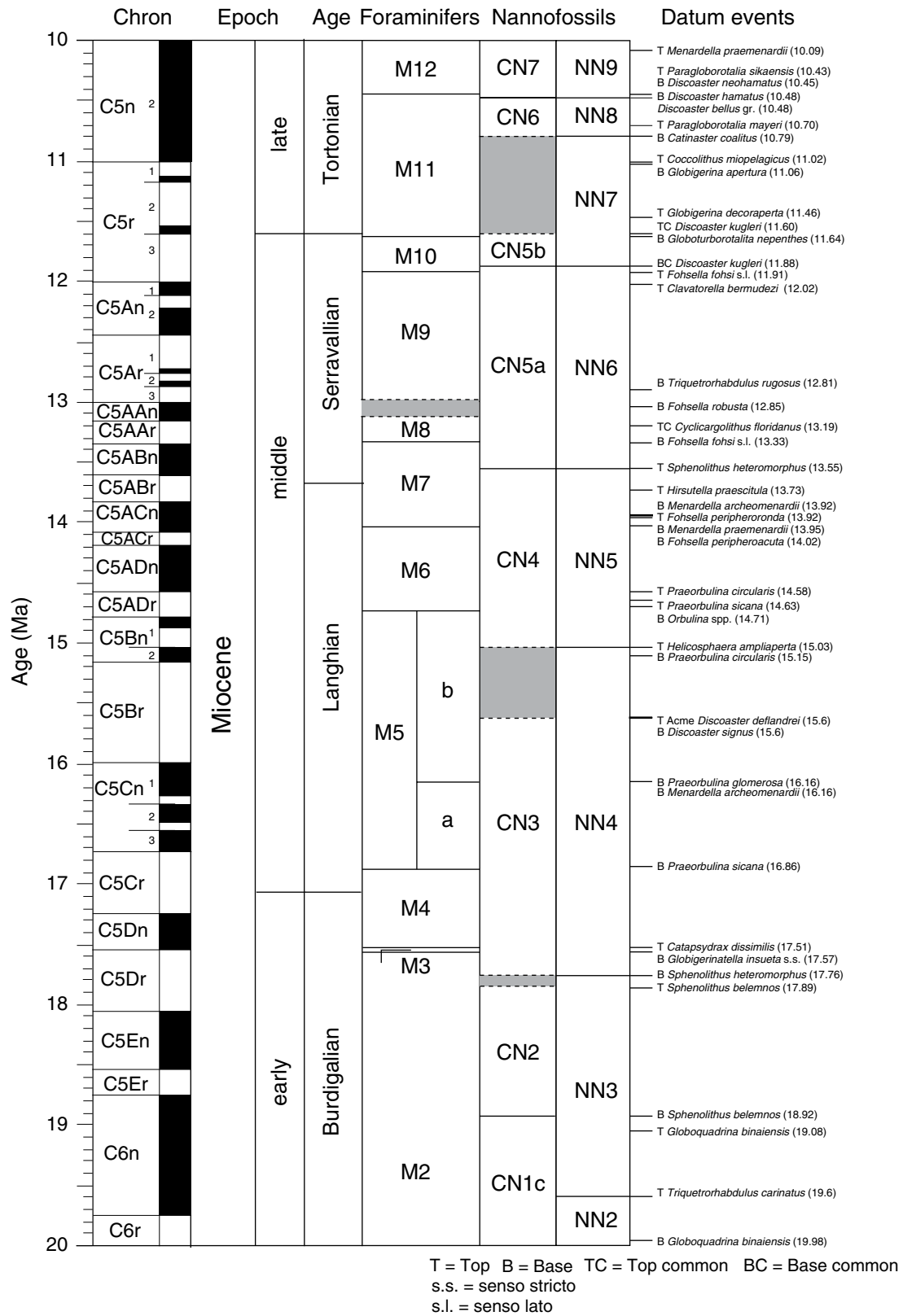


Figure 6, page 2.

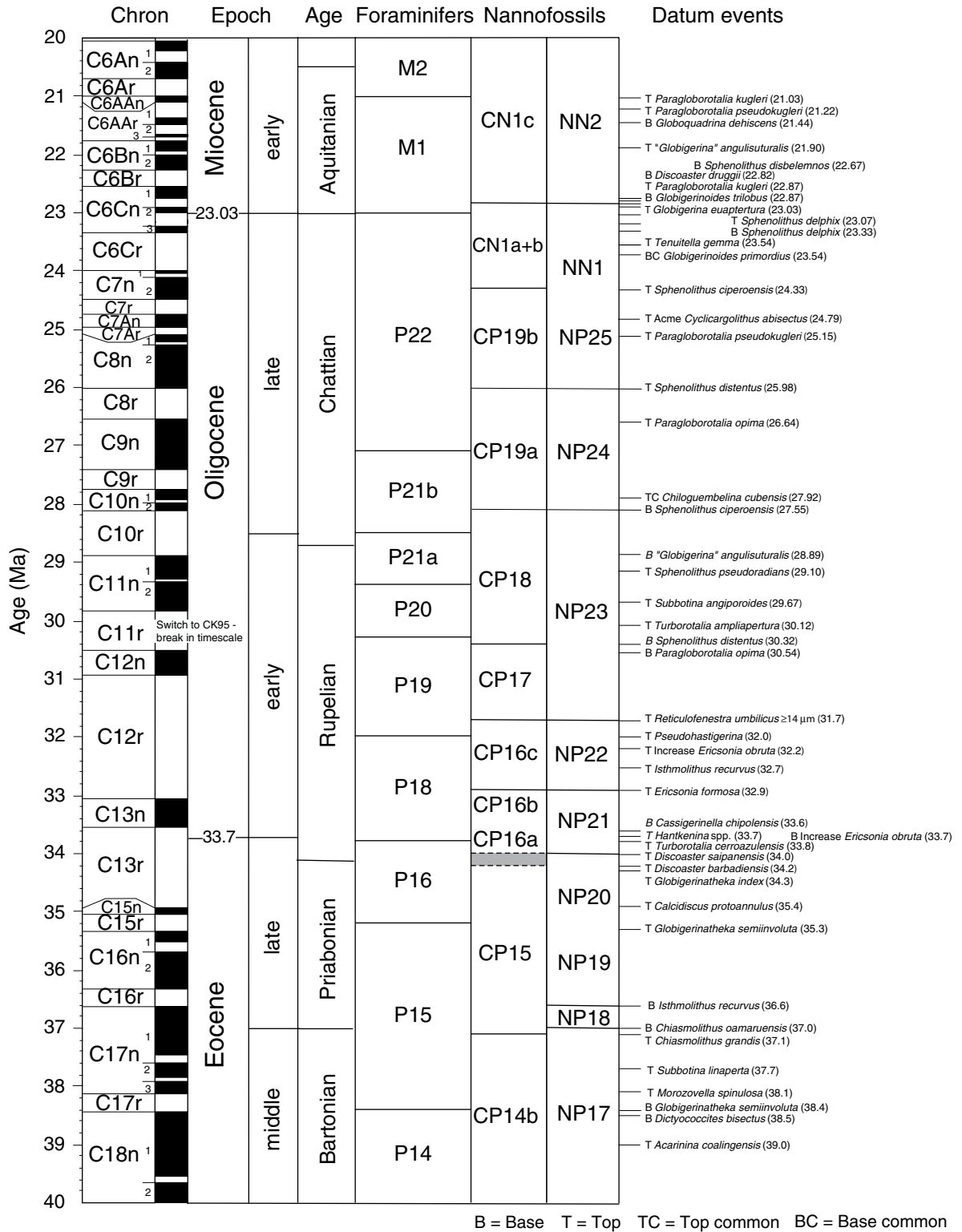


Figure 6, page 3.

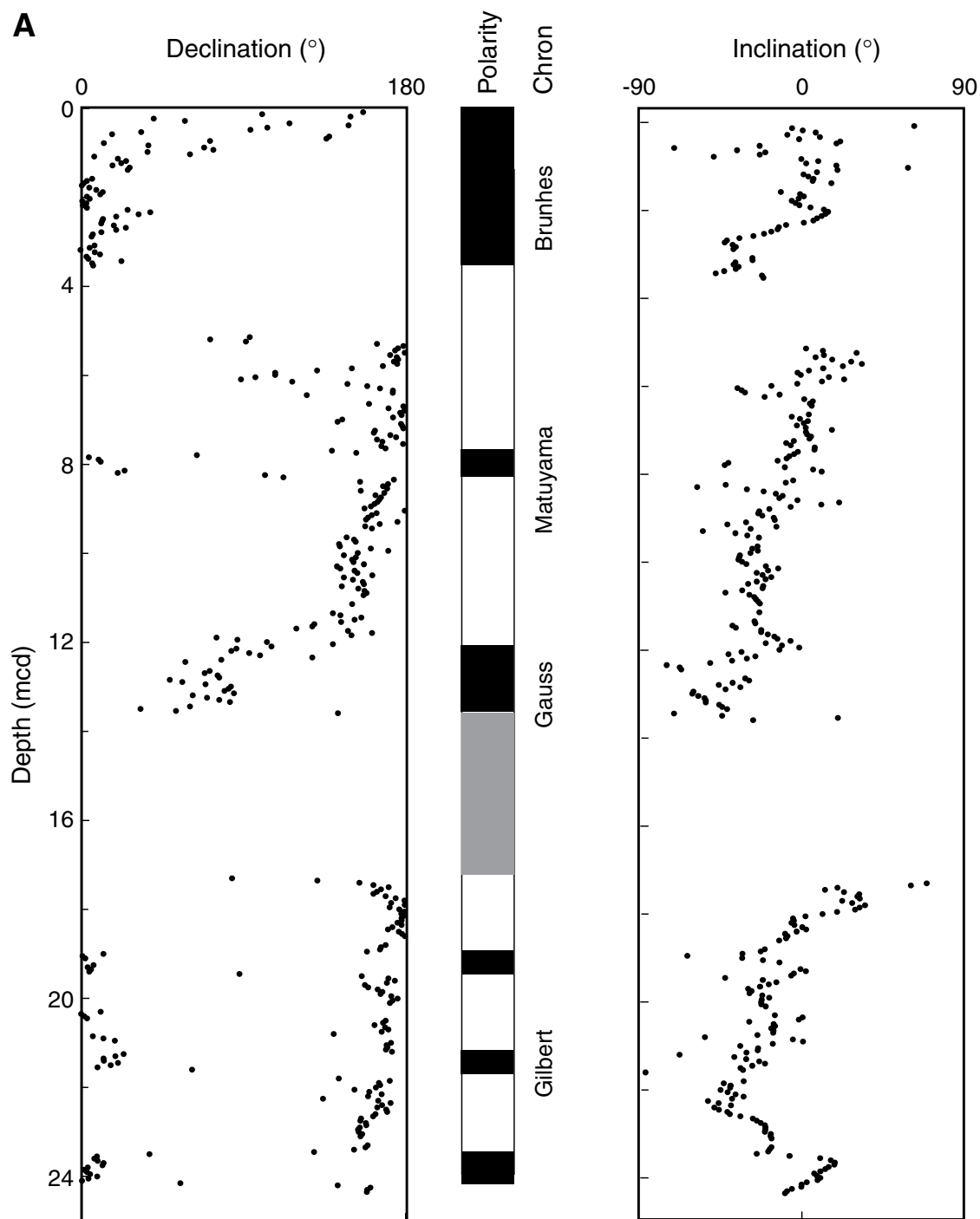


Figure 7. (page 1 of 3 pages) An example of geomagnetic data and interpretation. Composite magnetic stratigraphy at ODP Site 1218. Virtual geomagnetic pole (VGP) latitudes were obtained after partial AF demagnetization of continuous measurements at a peak field of 20 mT. Polarity column shows interpreted zones of normal (black) and reversed (white) magnetization, and gray intervals indicate zones with an uncertain polarity interpretation. A. Top 24 m of Hole 1218B, including cores not oriented with the Tensor tool. Note that both declination and inclination data are provided. B. Early Miocene-Pliocene section. Note the use of VGP (Virtual Geomagnetic Pole). VGP shows the latitude of the magnetic pole based on a single location rather than an average of locations; it is calculated from the declination, inclination, and the drillsite location. C. Early Oligocene-early Miocene section. From ODP Leg 199 Initial Reports volume, Site 1218 chapter, (http://www-odp.tamu.edu/publications/199_IR/chap_11/chap_11.htm)

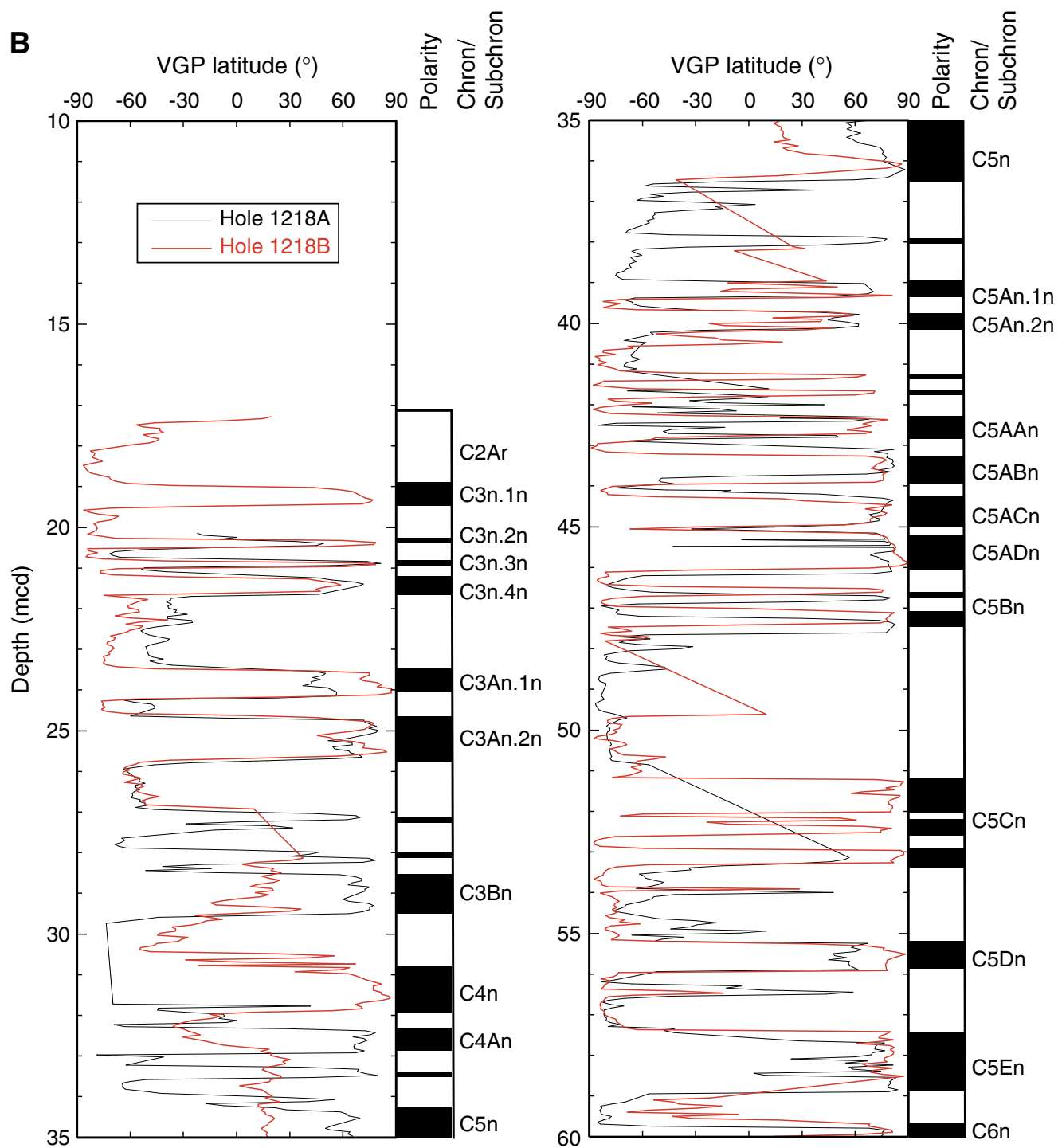


Figure 7 (page 2).

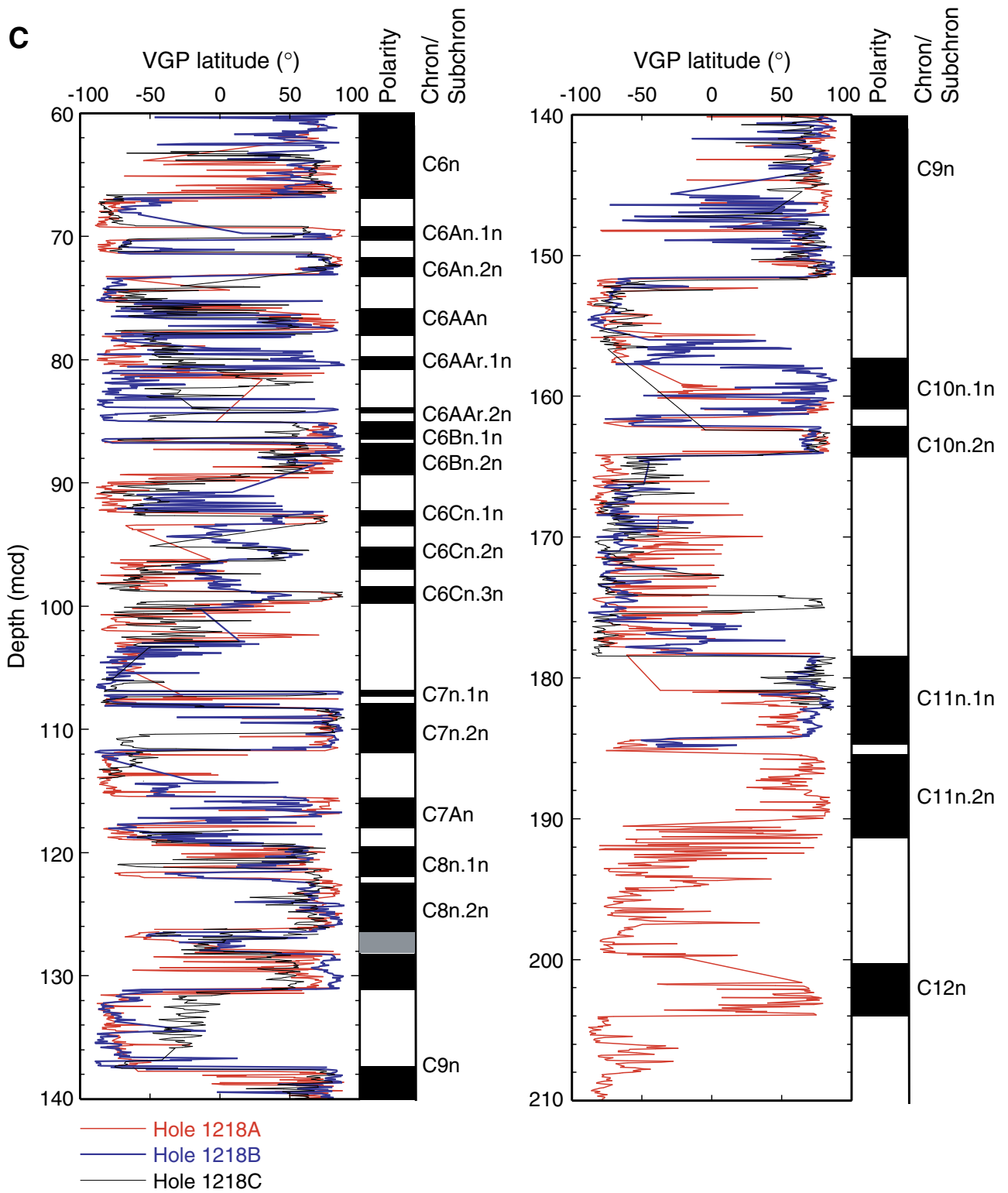


Figure 7 (page 3).

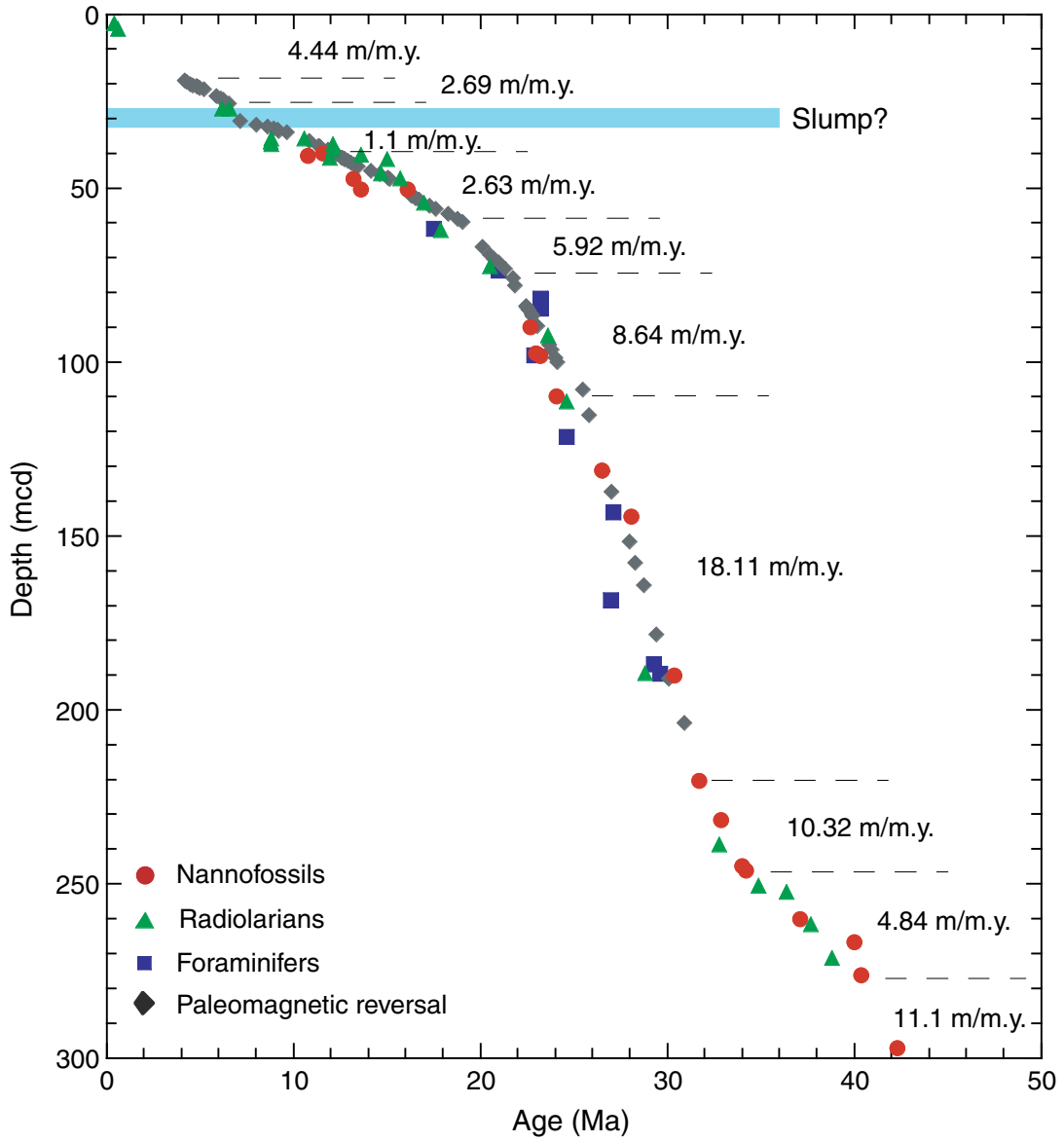


Figure 8. Age-depth plot of Site 1218 using paleomagnetic chron boundaries and biostratigraphic datums. LSRs (linear sedimentation rates) and chronostratigraphic markers. Data tables for the depths and ages of the paleomagnetic chrons and biostratigraphic datums are also available online at the following URL. From ODP Leg 199 Initial Reports volume, Site 1218 chapter. (http://www-odp.tamu.edu/publications/199_IR/chap_11/chap_11.htm)

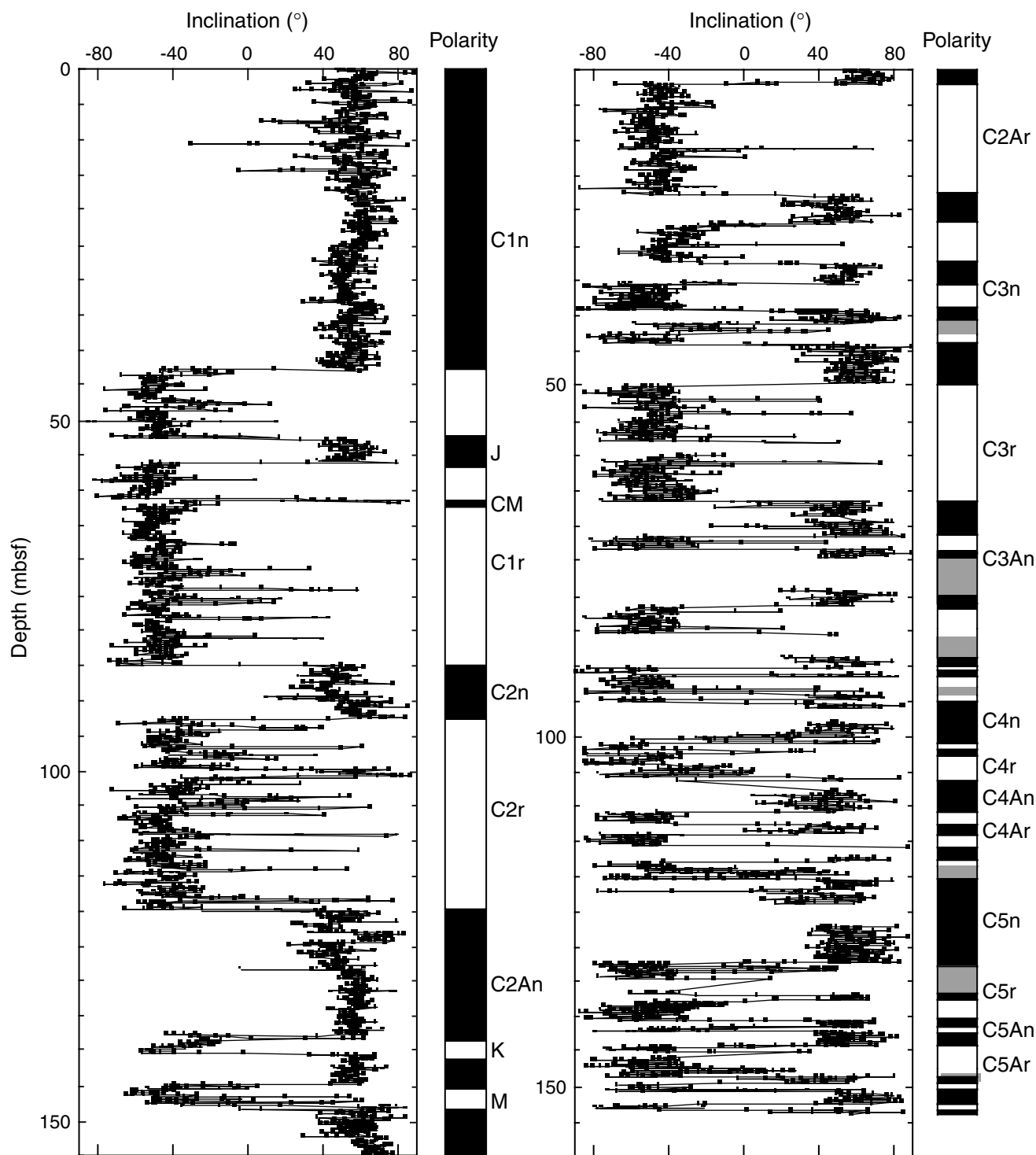


Figure 9. A second example of geomagnetic data and interpretation. Inclination after AF demagnetization at peak fields of 20 mT as measured with the shipboard pass-through magnetometer at Hole 1208A. The column at the right of each plot shows interpreted zones of normal (black) and reversed (white) polarity. Gray intervals indicate zones in which no polarity interpretation is possible. Polarity zones at the top of the section and certain polarity zones farther downsection are tentatively correlated to polarity chrons. From ODP Leg 198 Initial Reports volume, Site 1208 chapter. (http://www-odp.tamu.edu/publications/198_IR/chap_04/chap_04.htm)

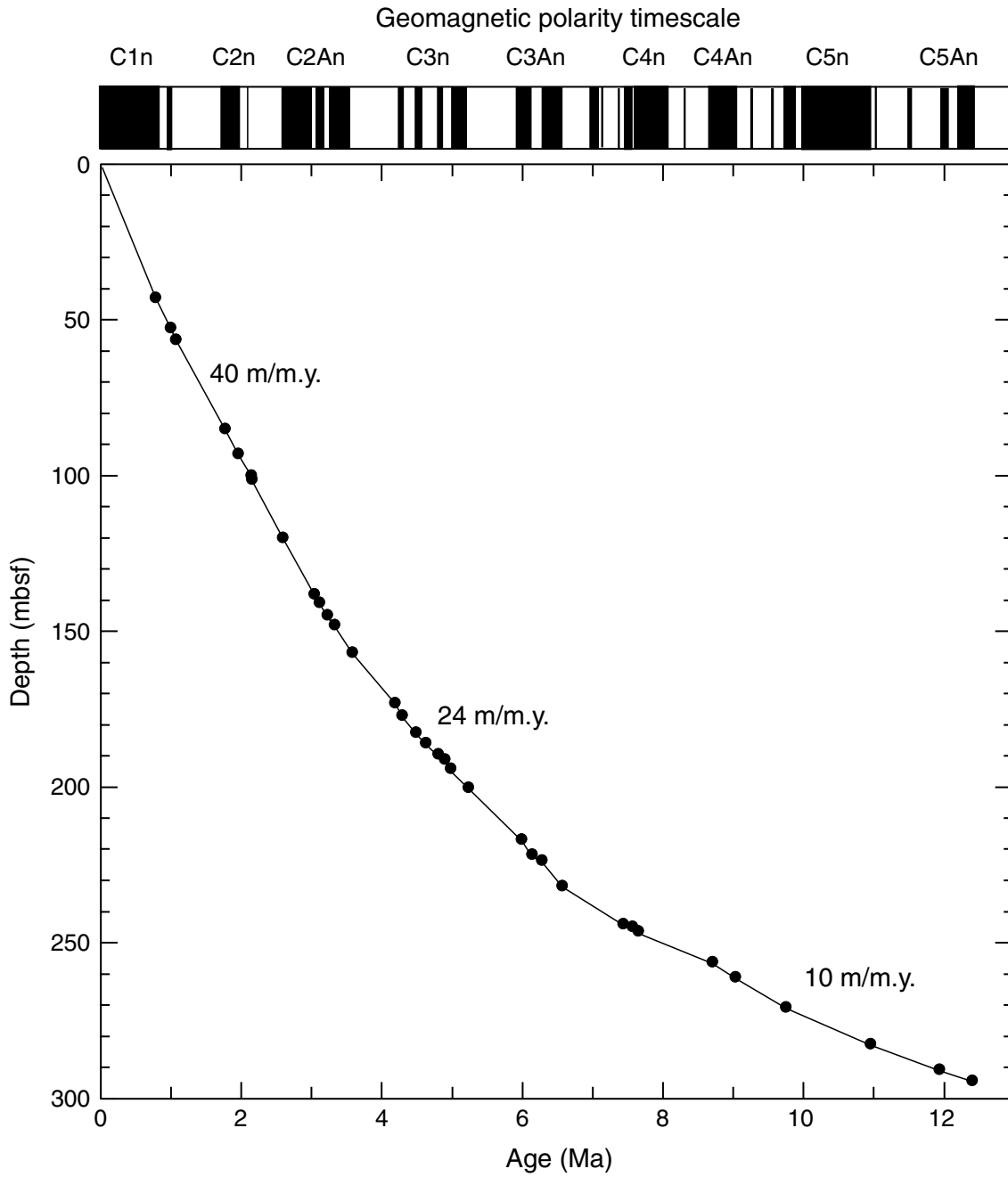


Figure 10. Age-depth curve for Site 1208 derived from the magnetic stratigraphy shown in Figure 9 using the geomagnetic polarity timescale of Cande and Kent (1995). Average sedimentation rates in meters per million years are also plotted. From ODP Leg 198 Initial Reports volume, Site 1208 chapter. (http://www-odp.tamu.edu/publications/198_IR/chap_04/chap_04.htm)

Paleomagnetic Stratigraphy Exercise

In this exercise, you will interpret the polarity chrons (geomagnetic reversal stratigraphy) for ODP Site 1237 in the southeast Pacific, located on the continental margin of Peru (16°0.421'S, 76°22.685'W; Figures 11 and 12). First, notice the latitude of this site. In the Northern Hemisphere, normal polarity is represented by positive inclination. Since this site is in the Southern Hemisphere, normal polarity will be represented by negative inclination (positive upwards, out of the Earth). Second, well-preserved magnetic data are either normal polarity or reversed polarity, and there have been many reversals during the past 30 million years represented by the sequence cored at Site 1237. You will need some independent means of age control in order to interpret the black and white stripes of normal and reversed polarity, respectively. Biostratigraphy based on the established sequence of first and last occurrences of microfossil species provides that first-order age control.

1. Using the Site 1237 biostratigraphic data provided (Table 1), interpret the polarity chrons for ODP Site 1237 (Holes 1237B, 1237C, and 1237D). The cored sequence is shown in 4 separate figures: Figure 13 (upper 100 meters composite depth, mcd); Figure 14 (100-200 mcd); Figure 15 (200-300 mcd); and Figure 16 (300-360 mcd). Construct your paleomagnetic stratigraphy to the right of the data presented in Figures 13-16. Color in segments representing normal polarity, and leave segments of reverse polarity blank (white).
2. Plot an age versus depth profile based on your paleomagnetic interpretations (you can plot it on the same graph as your biostratigraphic datums from the biostrat exercise). Use the graph paper provided. How well do the calcareous nannofossil datums compare with the polarity chron boundaries?

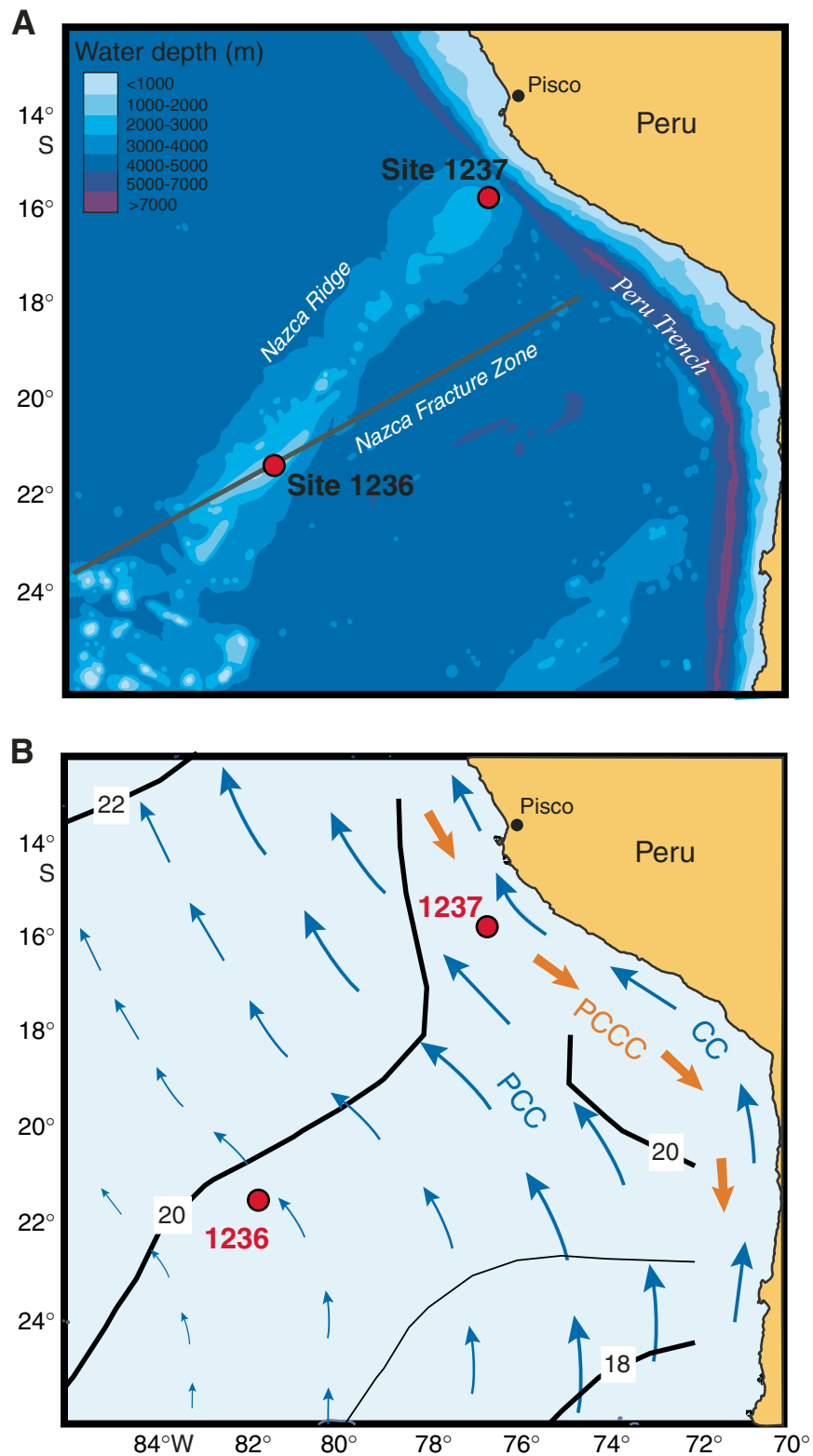


Figure 11. A. Locations of Sites 1236 and 1237 and bathymetry. B. Site locations and oceanographic features off Peru and northern Chile (CC = Coastal Current, PCCC = Peru-Chile Countercurrent, PCC = Peru-Chile Current), after Strub et al. (1998). Modern mean annual sea-surface temperatures (SSTs) (contours are in degrees Celsius, after Ocean Climate Laboratory, 1999). From ODP Leg 202 Initial Reports volume, Site 1237 chapter. (http://www-odp.tamu.edu/publications/202_IR/chap_08/chap_08.htm)

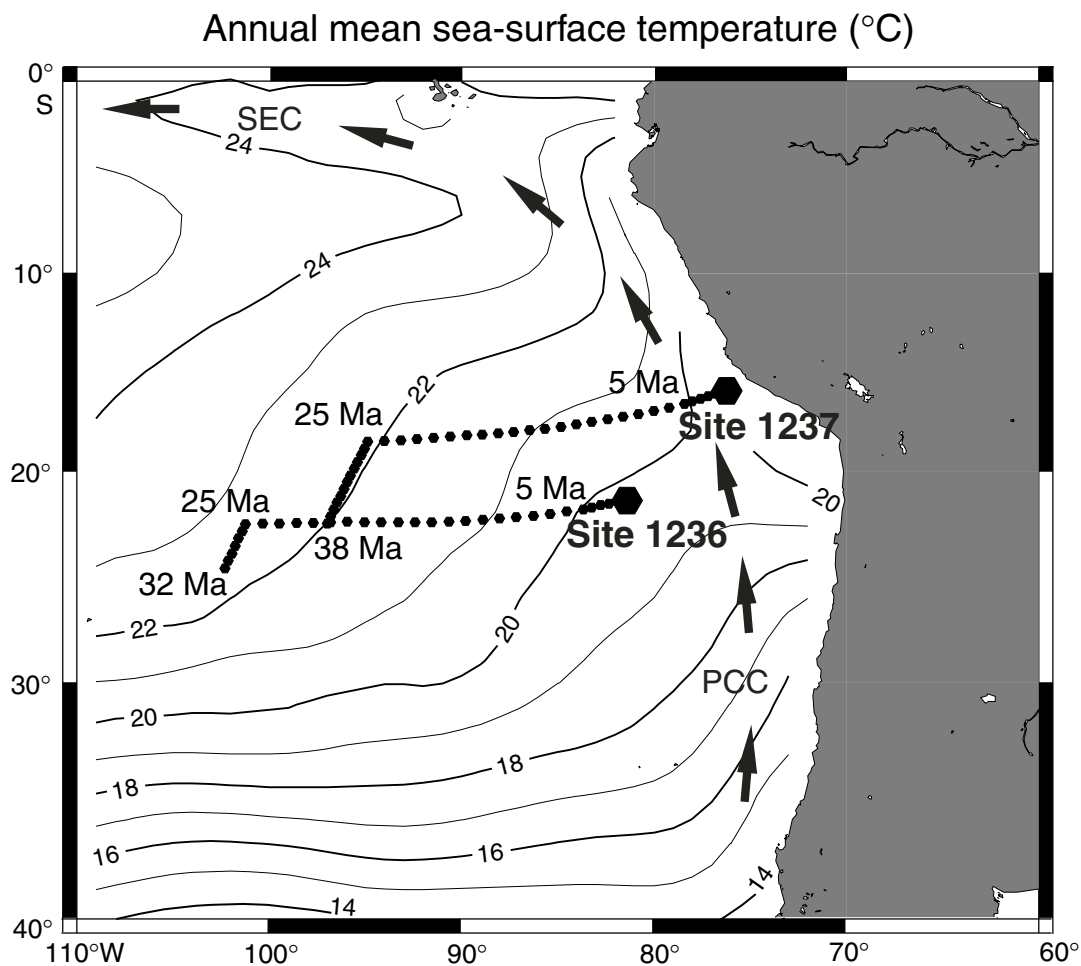


Figure 12. Tectonic backtrack of Site 1237, relative to a fixed South America. Poles of rotation are from Duncan and Hargraves (1984) and Pias et al. (1995). The dotted path represents positions in million-year increments. Numbers note ages (in millions of years) of changes in rate or direction of drift. Contours of modern mean annual sea-surface temperature are superimposed. PCC = Peru-Chile Current, SEC = South Equatorial Current). From ODP Leg 202 Initial Reports volume, Site 1237 chapter. (http://www-odp.tamu.edu/publications/202_IR/chap_08/chap_08.htm)

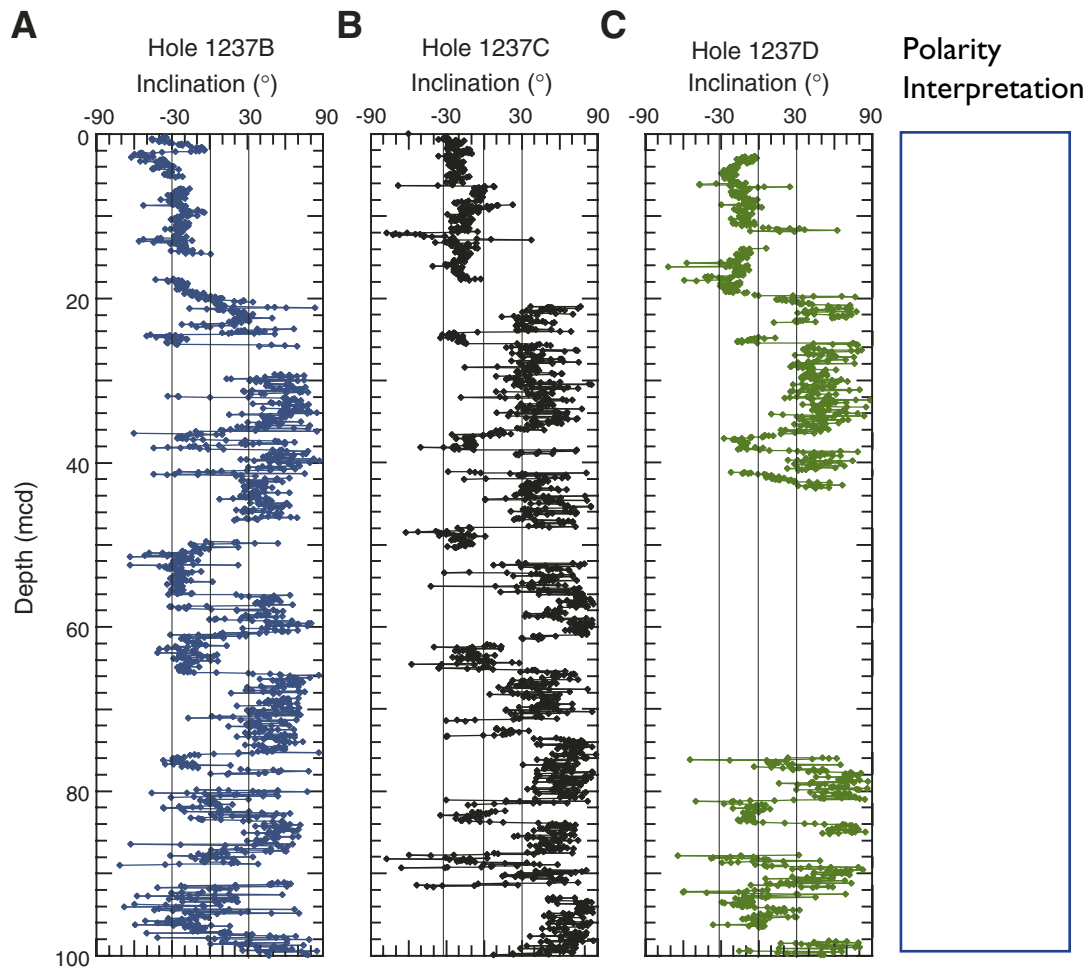


Figure 13. Inclination after demagnetization at peak alternating fields of 25 mT for the upper 100 mcd of (A) Hole 1237B, (B) Hole 1237C, and (C) Hole 1237D with the accompanying polarity interpretations. From ODP Leg 202 Initial Reports volume, Site 1237 chapter. (http://www-odp.tamu.edu/publications/202_IR/chap_08/chap_08.htm)

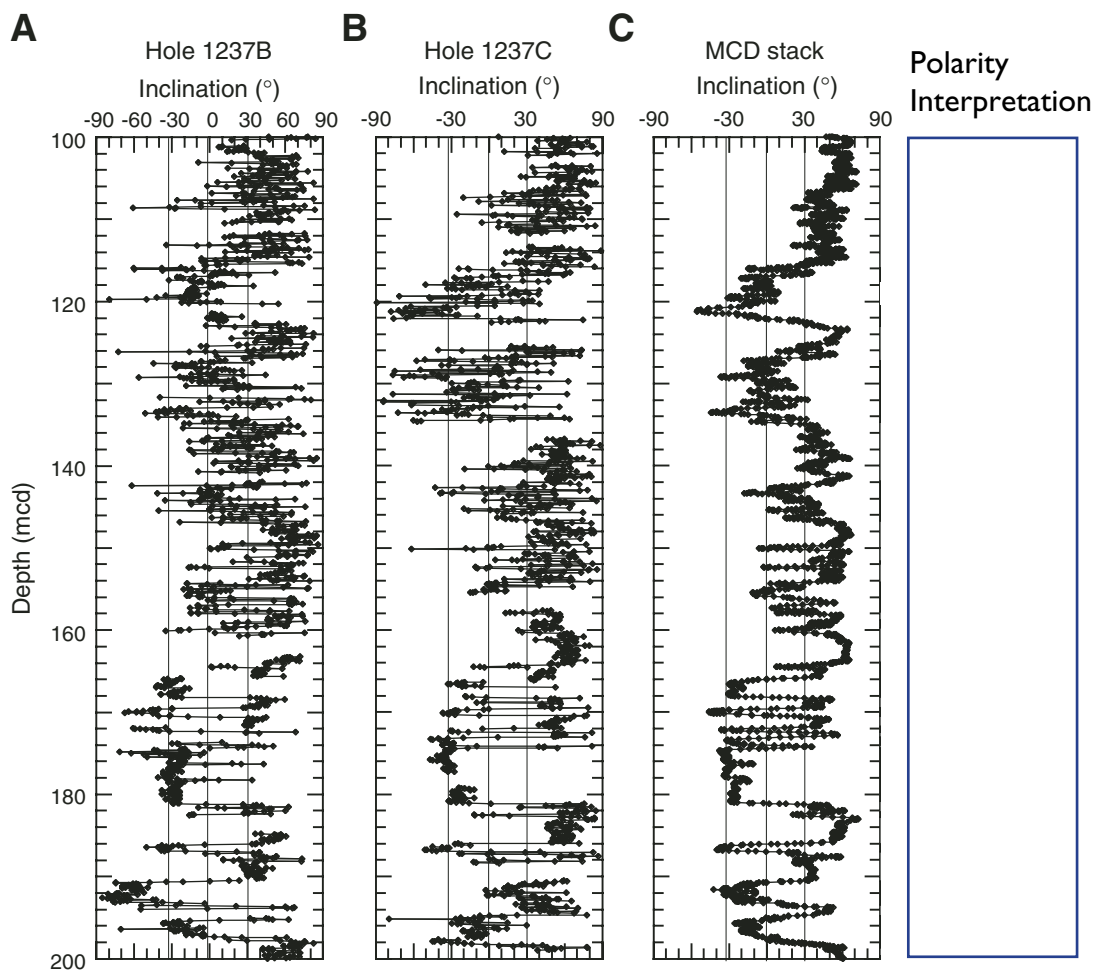


Figure 14. Inclination after demagnetization at peak alternating fields of 25 mT for the 100- to 200-mcd interval of (A) Hole 1237B, (B) Hole 1237C, and (C) the stacked and smoothed record with the accompanying polarity interpretations. From ODP Leg 202 Initial Reports volume, Site 1237 chapter. (http://www-odp.tamu.edu/publications/202_IR/chap_08/chap_08.htm)

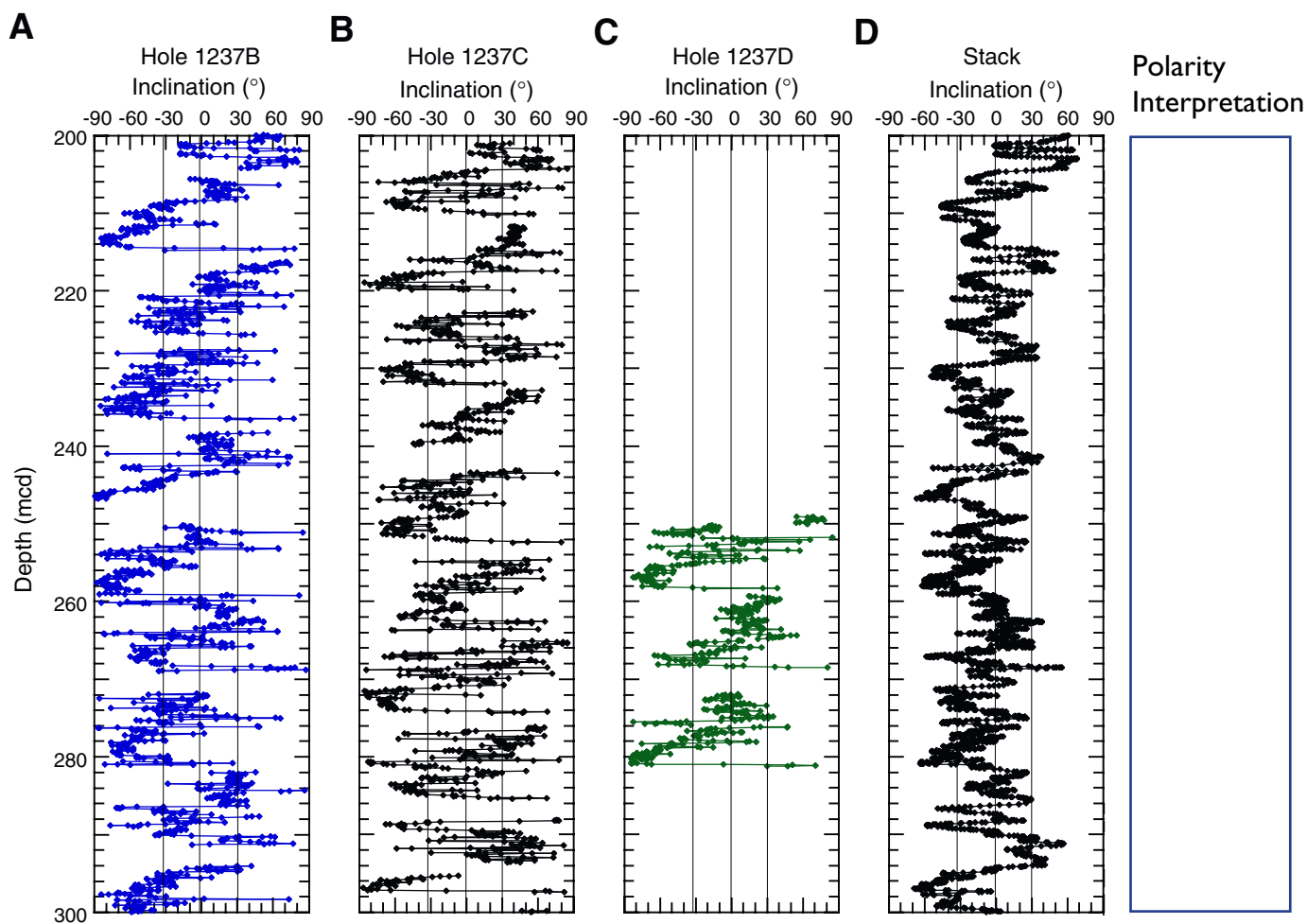


Figure 15. Inclination after demagnetization at peak alternating fields of 25 mT for the 200- to 300-mcd interval of (A) Hole 1237B, (B) Hole 1237C, (C) Hole 1237D, and (D) the stacked and smoothed record with the accompanying polarity interpretations. From ODP Leg 202 Initial Reports volume, Site 1237 chapter. (http://www-odp.tamu.edu/publications/202_IR/chap_08/chap_08.htm)

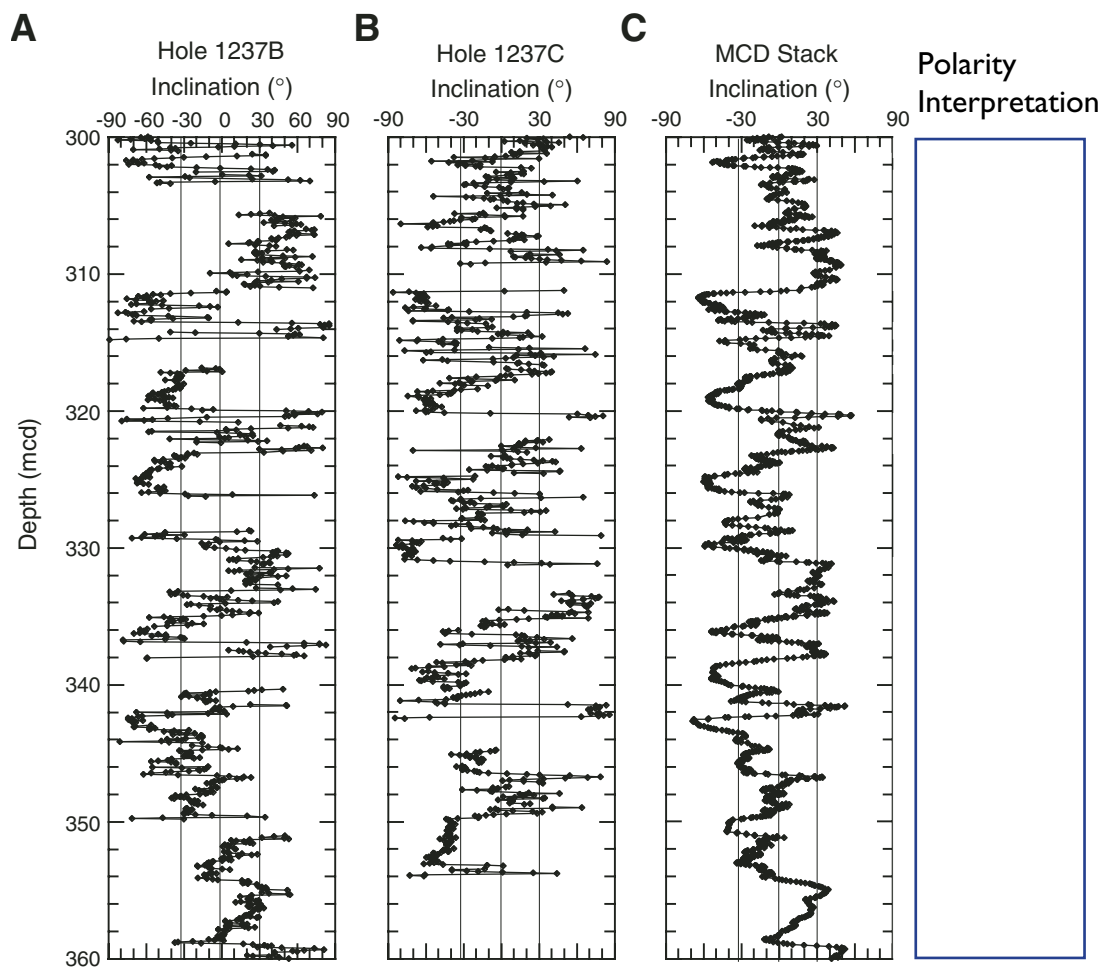


Figure 16. Inclination after demagnetization at peak alternating fields of 25 mT for the 300- to 360-mcd interval of (A) Hole 1237B, (B) Hole 1237C, and (C) the stacked and smoothed record with the accompanying polarity interpretations. From ODP Leg 202 Initial Reports volume, Site 1237 chapter. (http://www-odp.tamu.edu/publications/202_IR/chap_08/chap_08.htm)

Datum	Age (Ma)		Top sample (FO presence/LO absence)		Bottom sample (LO presence/FO absence)		Age (Ma)		Depth		
	Source	Minimum	Maximum	Core, section, interval (cm)	Depth (mbsf)	Core, section, interval (cm)	Depth (mbsf)	Average	Uncertainty (±)	Average (mbsf)	Uncertainty (±m)
FO <i>Emiliana huxleyi</i>	CN	0.26	0.26	202-1237B-1H-4, 75	5.26	202-1237B-1H-CC, 9	5.51	0.26	0.00	5.39	0.13
FO <i>Globorotalia hirsuta</i>	PF	0.45	0.45	1H-CC, 9	5.51	1H-CC, 9	15.47	0.45	0.00	10.49	10.07
LO <i>Pseudoemiliana lacunosa</i>	CN	0.46	0.46	2H-5, 75	12.28	2H-7, 40	14.94	0.46	0.00	13.61	12.76
LO <i>Nitzschia reinholdii</i>	D	0.62	0.62	2H-CC, 24	15.47	3H-5, 75	21.79	0.62	0.00	18.63	18.76
LO <i>Globorotalia tosaensis</i>	PF	0.65	0.65	1H-CC, 9	5.51	2H-CC, 24	15.47	0.65	0.00	10.49	10.07
LO <i>Nitzschia fossilis</i>	D	0.70	0.70	2H-CC, 24	15.47	3H-CC, 19	25.00	0.70	0.00	20.24	20.36
LO <i>Reticulolenestra asanoi</i>	CN	0.88	0.88	3H-4, 60	20.13	3H-5, 60	21.64	0.88	0.00	20.89	21.99
LO <i>Rhizosolenia matuyamai</i>	D	1.05	1.05	3H-3, 75	18.77	3H-5, 75	21.79	1.05	0.00	20.28	21.38
FO <i>Reticulolenestra asanoi</i>	CN	1.08	1.08	3H-CC, 19	25.00	4H-1, 75	25.25	1.08	0.00	25.13	27.83
FO <i>Rhizosolenia matuyamai</i>	D	1.18	1.18	3H-CC, 19	25.00	4H-1, 40	24.90	1.18	0.00	24.95	27.65
LO <i>Gephyrocapsa (large)</i>	CN	1.24	1.24	4H-1, 75	25.25	4H-2, 75	26.76	1.24	0.00	26.01	30.31
FO <i>Gephyrocapsa (large)</i>	CN	1.45	1.45	4H-2, 75	26.76	4H-3, 75	28.27	1.45	0.00	27.52	31.82
LO <i>Calcidiscus macintyreii</i>	CN	1.59	1.59	4H-3, 75	28.27	4H-6, 75	32.81	1.59	0.00	30.54	34.84
LO <i>Globigerinoides extremus</i>	PF	1.77	1.77	2H-CC, 24	15.47	3H-CC, 19	25.00	1.77	0.00	20.24	20.36
LO <i>Discoaster brouweri</i>	CN	1.96	1.96	4H-CC, 20	34.55	5H-1, 75	34.75	1.96	0.00	34.65	38.44
FO <i>Fragilaropsis dololus</i>	D	2.00	2.00	4H-3, 40	27.92	4H-6, 40	32.46	2.00	0.00	30.19	34.49
LO <i>Globorotalia punctulata</i>	PF	2.41	2.41	3H-CC, 19	25.00	4H-CC, 20	34.55	2.41	0.00	29.78	32.48
LO <i>Thalassiosira convexa</i> s.l.	D	2.41	2.41	4H-6, 40	32.46	4H-CC, 20	34.55	2.41	0.00	33.51	37.81
LO <i>Discoaster pentaradiatus</i>	CN	2.44	2.44	5H-6, 75	42.30	5H-CC, 22	44.02	2.44	0.00	43.16	46.43
LO <i>Discoaster surculus</i>	CN	2.61	2.61	5H-6, 75	42.30	5H-CC, 22	44.02	2.61	0.00	43.16	46.43
LO <i>Discoaster tamalis</i>	CN	2.76	2.76	6H-1, 75	44.25	6H-2, 75	45.76	2.76	0.00	45.01	50.73
LO <i>Nitzschia jouseae</i>	D	2.77	2.77	6H-1, 75	44.25	6H-2, 22	45.23	2.77	0.00	44.74	50.46
LO <i>Dentoglobigerina altispira</i>	PF	3.09	3.09	5H-CC, 22	44.02	6H-CC, 30	53.51	3.09	0.00	48.77	53.26
LO <i>Sphaeroidinellopsis seminula</i>	PF	3.12	3.12	6H-CC, 30	53.51	7H-CC, 19	62.80	3.12	0.00	58.16	63.80
FO <i>Rhizosolenia praeborgonii</i> s.l.	D	3.17	3.17	7H-1, 110	54.10	7H-3, 73	56.74	3.17	0.00	55.42	60.99
FO <i>Sphaeroidinella dehiscentis</i>	PF	3.25	3.25	6H-CC, 30	53.51	7H-CC, 19	62.80	3.25	0.00	58.16	63.80
LO <i>Globorotalia plesiotumida</i>	PF	3.77	3.77	7H-CC, 19	62.80	8H-CC, 39	72.66	3.77	0.00	67.73	73.38
LO <i>Reticulolenestra pseudoubillicus</i>	CN	3.80	3.80	8H-1, 75	63.25	8H-2, 78	64.79	3.80	0.00	64.02	69.74
FO <i>Pseudoemiliana lacunosa</i>	CN	4.00	4.00	9H-3, 78	75.78	9H-4, 75	77.27	4.00	0.00	76.53	83.91
LO <i>Globorotalia nepenthes</i>	PF	4.20	4.20	8H-CC, 39	72.66	9H-CC, 20	81.86	4.20	0.00	77.26	83.81
LO <i>Sphaeroidinellopsis kochi</i>	PF	4.53	4.53	8H-CC, 39	72.66	9H-CC, 20	81.86	4.53	0.00	77.26	83.81
LO <i>Nitzschia cylindrica</i>	D	4.88	4.88	8H-CC, 39	72.66	9H-6, 30	79.83	4.88	0.00	76.25	82.79
FO <i>Nitzschia jouseae</i>	D	5.12	5.12	9H-CC, 20	81.86	10H-CC, 10	91.29	5.12	0.00	86.58	94.87
LO <i>Discoaster quinqueramus</i>	CN	5.56	5.56	11H-4, 75	96.28	11H-5, 75	97.79	5.56	0.00	97.04	106.71
FO <i>Thalassiosira oestrupii</i>	D	5.64	5.64	11H-CC, 25	101.10	12H-1, 22	100.72	5.64	0.00	100.91	111.13
FO <i>Globorotalia tumida</i>	PF	5.82	5.82	10H-CC, 10	91.29	11H-CC, 25	101.10	5.82	0.00	96.20	105.64
LO <i>Nitzschia miocenica</i> s.s.	D	6.08	6.08	12H-4, 38	105.40	13H-CC, 1	119.75	6.08	0.00	112.58	123.49
FO <i>Globorotalia margaritae</i>	PF	6.09	6.09	11H-CC, 25	101.10	12H-CC, 18	109.81	6.09	0.00	105.46	115.68
FO <i>Globigerinoides conglobatus</i>	PF	6.20	6.20	12H-CC, 18	109.81	13H-CC, 1	119.75	6.20	0.00	114.78	125.69
FO <i>Pulletanica primalis</i>	PF	6.40	6.40	12H-CC, 18	109.81	13H-CC, 1	119.75	6.40	0.00	114.78	125.69
FO <i>Thalassiosira convexa</i> v. <i>aspinosa</i>	D	6.57	6.57	13H-CC, 1	119.75	14H-3, 34	122.86	6.57	0.00	121.31	132.71
LO Absence interval <i>Reticulolenestra pseudoubillicus</i> > 7 µm	CN	6.80	6.80	14H-CC, 26	129.40	15H-1, 75	129.40	6.80	0.00	129.58	141.73
FO <i>Globorotalia conomiozea</i>	PF	7.12	7.12	13H-CC, 1	119.75	14H-CC, 26	129.40	7.12	0.00	124.58	135.98
FO <i>Amaurillus primus</i>	CN	7.24	7.24	15H-3, 75	132.77	15H-5, 75	135.79	7.24	0.00	134.28	146.83
FO <i>Nitzschia miocenica</i> s.l.	D	7.30	7.30	13H-CC, 1	119.75	14H-3, 34	122.86	7.30	0.00	121.31	132.71
FO <i>Nitzschia reinholdii</i>	D	7.64	7.64	14H-CC, 26	129.40	15H-CC, 1	138.66	7.64	0.00	134.03	146.18

Table 1. (two pages) Age-Depth control points for ODP Hole 1237B. These are the biostratigraphic datums (microfossil first and last occurrence datums; FOs and LOs) used to calibrate the paleomagnetic record of Site 1237. This image is scanned from the ODP Leg 202 Initial Reports volume, Site 1237 site chapter (choose pdf version rather than online html version), http://www-odp.tamu.edu/publications/202_IR/chap_08/chap_08.htm.

Datum	Source	Age (Ma)		Top sample (FO presence/LO absence)		Bottom sample (LO presence/FO absence)		Age (Ma)		Depth		
		Minimum	Maximum	Core, section, interval (cm)	Depth (mbsf)	Core, section, interval (cm)	Depth (mbsf)	Average	Uncertainty (±)	Average (mbsf)	Uncertainty (±m)	
FO <i>Globborotalia plesiotumida</i>	PF	8.58	8.58	15H-CC, 1	138.66	16H-CC, 12	148.21	8.58	0.00	143.44	156.06	4.78
FO absence interval <i>Reticulofenestra pseudoumbilicus</i> >7µm	CN	8.85	8.85	17H-1, 75	148.75	17H-1, 86	148.86	8.85	0.00	148.81	163.61	0.06
LO <i>Discaster hamatus</i>	CN	9.40	9.40	17H-5, 75	154.78	17H-6, 75	156.28	9.40	0.00	155.53	170.33	0.75
FO <i>Neogloboquadrina acostaensis</i>	PF	9.82	9.82	17H-1, 98	148.98	17H-CC, 21	158.00	9.82	0.00	153.49	168.29	4.51
LO <i>Coccolithus miopelagicus</i>	CN	10.40	10.40	18H-4, 75	162.43	18H-5, 75	163.94	10.40	0.00	163.19	178.92	0.75
FO <i>Globborotalia nepanthes</i>	PF	11.19	11.19	18H-CC, 1	166.89	19H-CC, 13	176.81	11.19	0.00	171.85	188.39	4.96
LO <i>Coronocylus nitescens</i>	CN	12.43	12.43	19H-3, 75	170.78	19H-4, 75	172.29	12.43	0.00	171.54	188.89	0.75
LO <i>Cyclargolithus floridanus</i>	CN	11.6	13.19	19H-5, 75	173.80	19H-6, 75	175.30	12.40	0.80	174.55	191.90	0.75
LO <i>Globborotalia fohsi</i> s.l.	PF	11.68	11.68	18H-CC, 1	166.89	19H-CC, 13	176.81	11.68	0.00	171.85	188.39	4.96
LO <i>Calcidiscus premacintyrei</i>	CN	12.4	12.4	19H-6, 75	175.30	19H-7, 40	176.46	12.40	0.00	175.88	193.23	0.58
FO <i>Globborotalia fohsi</i> s.l.	PF	13.42	13.42	19H-CC, 13	176.81	20H-CC, 24	186.41	13.42	0.00	181.61	199.36	4.80
LO <i>Sphenolithus heteromorphus</i>	CN	13.57	13.57	20H-7, 40	185.95	20H-CC, 24	186.41	13.57	0.00	186.18	204.33	0.23
LO <i>Globborotalia archeomenardii</i>	PF	14.2	14.2	19H-CC, 13	176.81	20H-CC, 24	186.41	14.20	0.00	181.61	199.36	4.80
LO <i>Globborotalia perpheroranda</i>	PF	14.6	14.6	20H-CC, 24	186.41	21H-CC, 14	195.79	14.60	0.00	191.10	209.78	4.69
FO <i>Globborotalia perpheroranda</i>	PF	14.80	14.80	21H-CC, 14	195.79	22H-CC, 1	205.44	14.80	0.00	200.62	220.39	4.83
FO <i>Globborotalia praemenardii</i>	PF	14.9	14.9	21H-CC, 14	195.79	22H-CC, 1	205.44	14.90	0.00	200.62	220.39	4.83
FO <i>Globborotalia miozea</i>	PF	15.9	15.9	21H-CC, 14	195.79	22H-CC, 1	205.44	15.90	0.00	200.62	220.39	4.83
FO <i>Globbigerinoides diminitus</i>	PF	16.1	16.1	22H-CC, 1	205.44	23H-CC, 16	214.67	16.10	0.00	210.06	231.31	4.62
FO <i>Globborotalia birnageae</i>	PF	16.7	16.7	23H-CC, 16	214.67	24H-CC, 10	224.17	16.70	0.00	219.42	242.17	4.75
LO <i>Globborotalia semivera</i>	PF	17.30	17.30	23H-CC, 16	214.67	24H-CC, 10	224.17	17.30	0.00	219.42	242.17	4.75
LO <i>Catapsydrax dissimilis</i>	PF	17.30	17.30	23H-CC, 16	214.67	24H-CC, 10	224.17	17.30	0.00	219.42	242.17	4.75
FO <i>Calcidiscus premacintyrei</i>	CN	17.40	17.40	23H-3, 75	208.77	23H-4, 75	210.28	17.40	0.00	209.53	231.68	0.75
FO <i>Sphenolithus heteromorphus</i>	CN	18.20	18.20	23H-CC, 16	214.67	24H-1, 75	215.25	18.20	0.00	214.96	237.71	0.29
LO <i>Sphenolithus belemnos</i>	CN	18.50	18.50	23H-CC, 16	214.67	24H-1, 75	215.25	18.50	0.00	214.96	237.71	0.29
LO <i>Globoquadrina binaiensis</i>	PF	19.10	19.10	24H-CC, 10	224.17	25H-CC, 10	233.68	19.10	0.00	228.93	253.50	4.76
FO <i>Sphenolithus belemnos</i>	CN	19.20	19.20	24H-6, 75	222.81	24H-7, 40	223.96	19.20	0.00	223.39	246.74	0.57
LO <i>Paraglobborotalia kugleri</i>	PF	21.50	21.50	25H-CC, 10	233.68	26H-CC, 9	243.48	21.50	0.00	238.58	264.31	4.90
LO <i>Globborotalia angulifuturalis</i>	PF	21.60	21.60	25H-CC, 10	233.68	26H-CC, 9	243.48	21.60	0.00	238.58	264.31	4.90
FO <i>Globoquadrina binaiensis</i>	PF	22.10	22.10	27H-CC, 14	252.80	28H-CC, 16	262.48	22.10	0.00	257.64	286.40	4.84
FO <i>Globoquadrina dehiscens</i>	PF	23.20	23.20	27H-CC, 14	252.80	28H-CC, 16	262.48	23.20	0.00	257.64	286.40	4.84
FO <i>Globbigerinoides trilobus</i>	PF	23.40	23.40	28H-CC, 16	262.48	29H-CC, 15	271.95	23.40	0.00	267.22	297.55	4.74
LO <i>Reticulofenestra bisecta</i>	CN	23.90	23.90	29H-4, 75	267.27	29H-5, 75	268.78	23.90	0.00	268.03	299.64	0.75
FO <i>Globbigerinoides primordius</i> common	PF	24.30	24.30	29H-CC, 15	271.95	30H-CC, 0	281.24	24.30	0.00	276.60	309.21	4.65
LO <i>Zygrhabdolithus bijugatus</i>	CN	24.50	24.50	29H-5, 75	268.78	29H-5, 75	268.78	24.50	0.00	268.78	300.39	0.00
LO <i>Sphenolithus ciproensis</i>	CN	24.75	24.75	29H-5, 75	268.78	29H-5, 75	268.78	24.75	0.00	268.78	300.39	0.00
FO <i>Globbigerinoides primordius</i>	PF	26.70	26.70	30H-CC, 0	281.24	31H-CC, 16	291.07	26.70	0.00	286.16	320.67	4.91
LO <i>Sphenolithus distentus</i>	CN	27.5	27.5	31H-7, 40	290.47	31H-CC, 16	291.07	27.50	0.00	290.77	326.18	0.30
LO <i>Sphenolithus predistentus</i>	CN	27.5	27.5	31H-CC, 16	291.07	32H-1, 75	291.25	27.50	0.00	291.16	327.77	0.09
LO <i>Sphenolithus pseudoradians</i>	CN	29.1	29.1	33H-5, 75	306.78	33H-6, 75	308.29	29.10	0.00	307.54	347.40	0.75
FO <i>Globborotalia angulifuturalis</i>	PF	29.40	29.40	31H-CC, 16	291.07	32H-CC, 25	300.54	29.40	0.00	295.81	332.42	4.74
FO <i>Sphenolithus ciproensis</i>	CN	29.9	29.9	33H-5, 75	306.78	33H-6, 75	308.29	29.90	0.00	307.54	347.40	0.75
LO <i>Subbotina angiporoidea</i>	PF	30.00	30.00	32H-CC, 25	300.54	33H-6, 75	308.29	30.00	0.00	304.42	355.28	3.88
LO <i>Turborotalia ampliapertura</i>	PF	30.30	30.30	32H-CC, 25	300.54	33H-6, 75	308.29	30.30	0.00	304.42	355.16	3.88

Notes: FO = first occurrence, LO = last occurrence. CN = calcareous nannofossils, PF = planktonic foraminifers, D = diatoms.

Table 1, page two.

